STAR

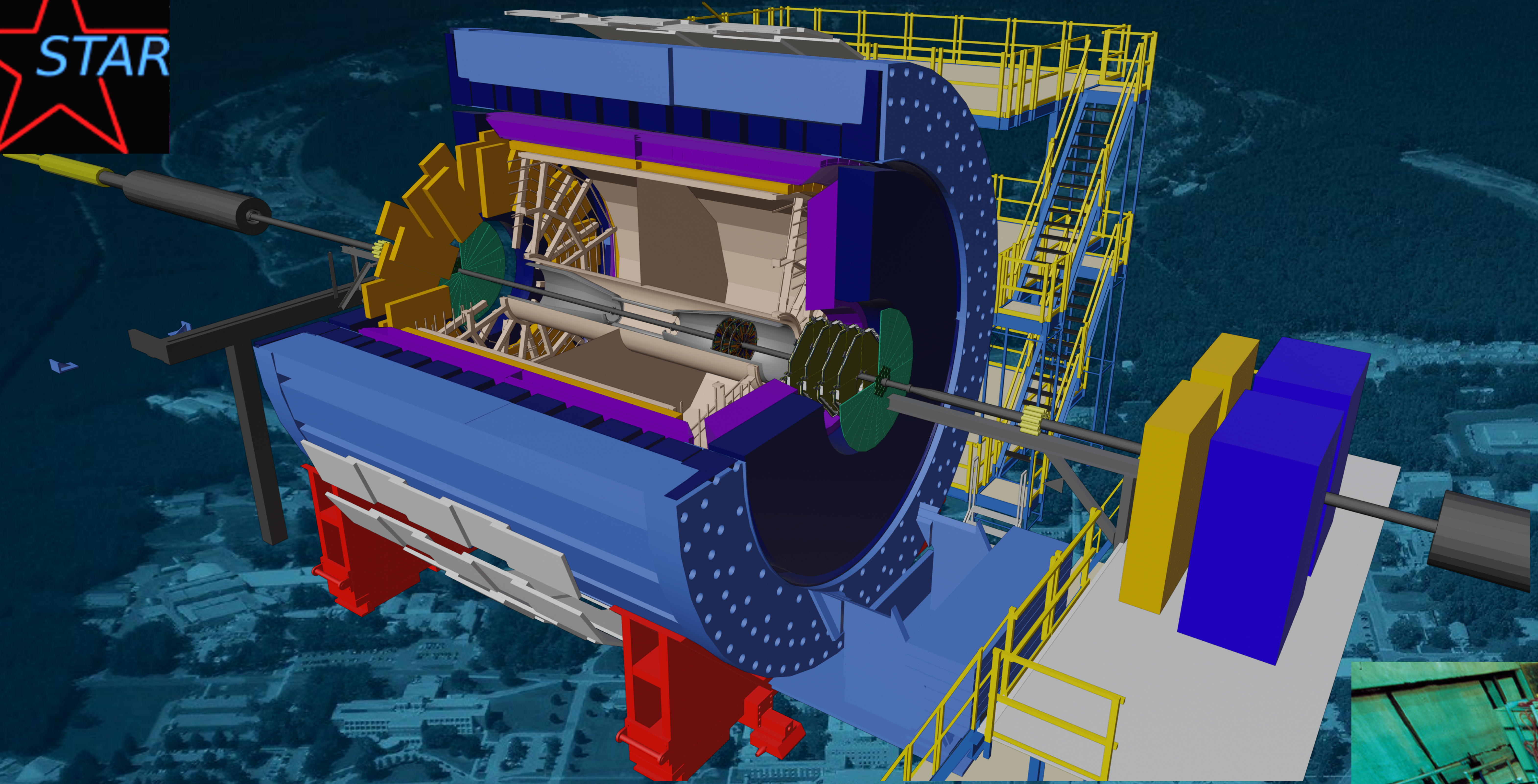

Brookhaven National Laboratory

U.S. DEPARTMENT OF ENERGY

PHENIX

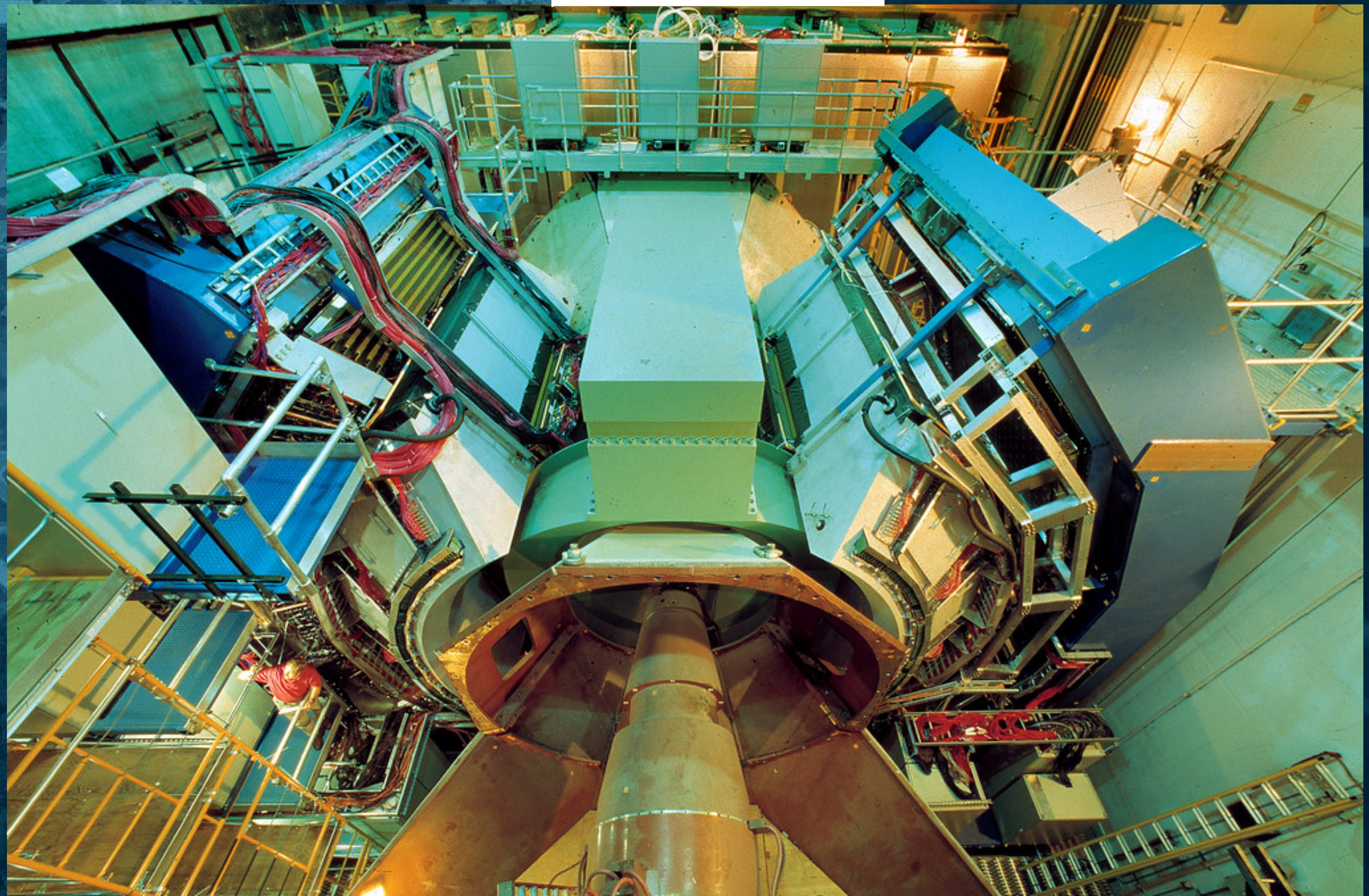

RHIC Results

Michal Šumbera

(Nuclear Physics Institute CAS)

sumbera@ujf.cas.cz

RHIC physics program at glance

1. Phase diagram of hot and dense QCD matter

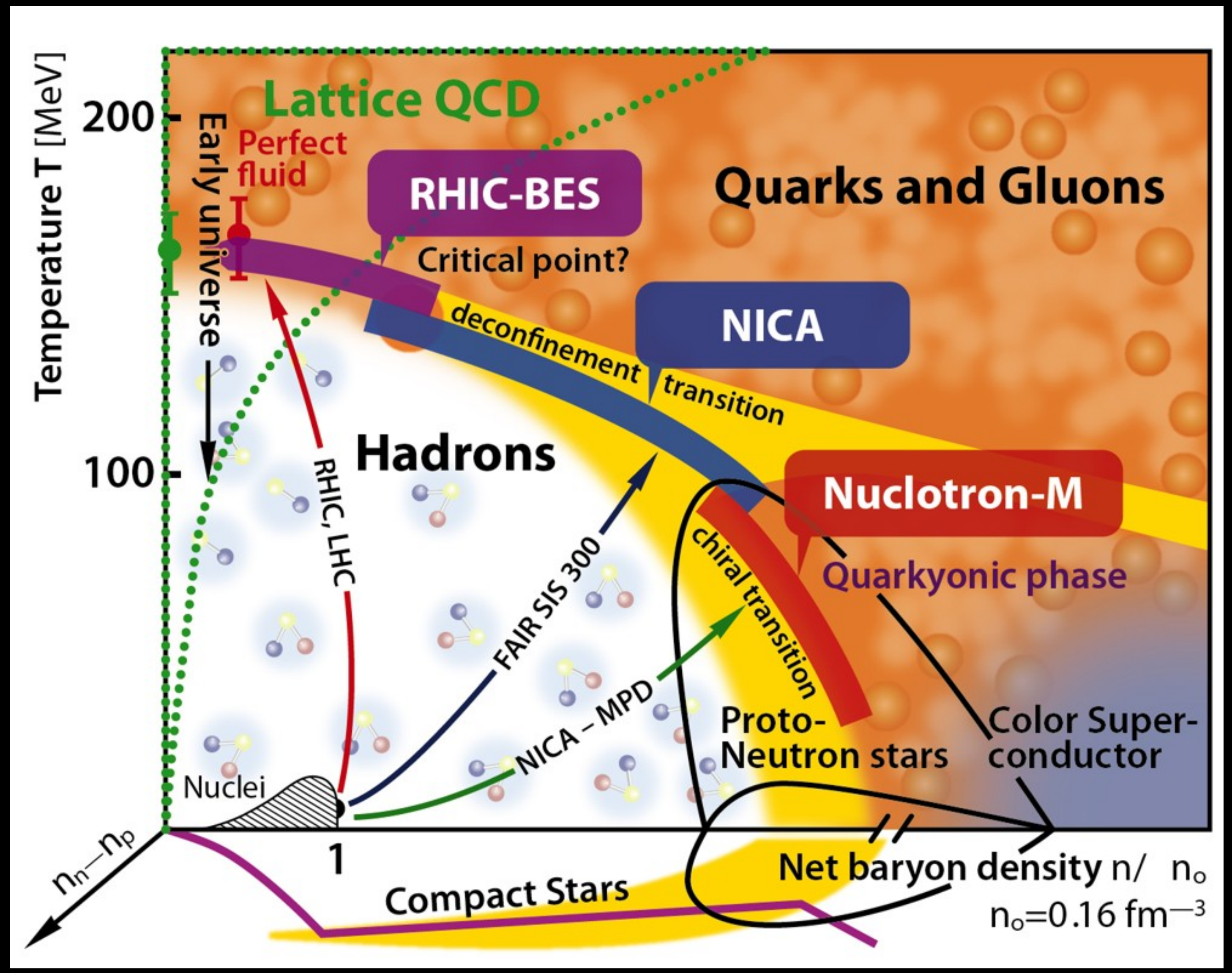

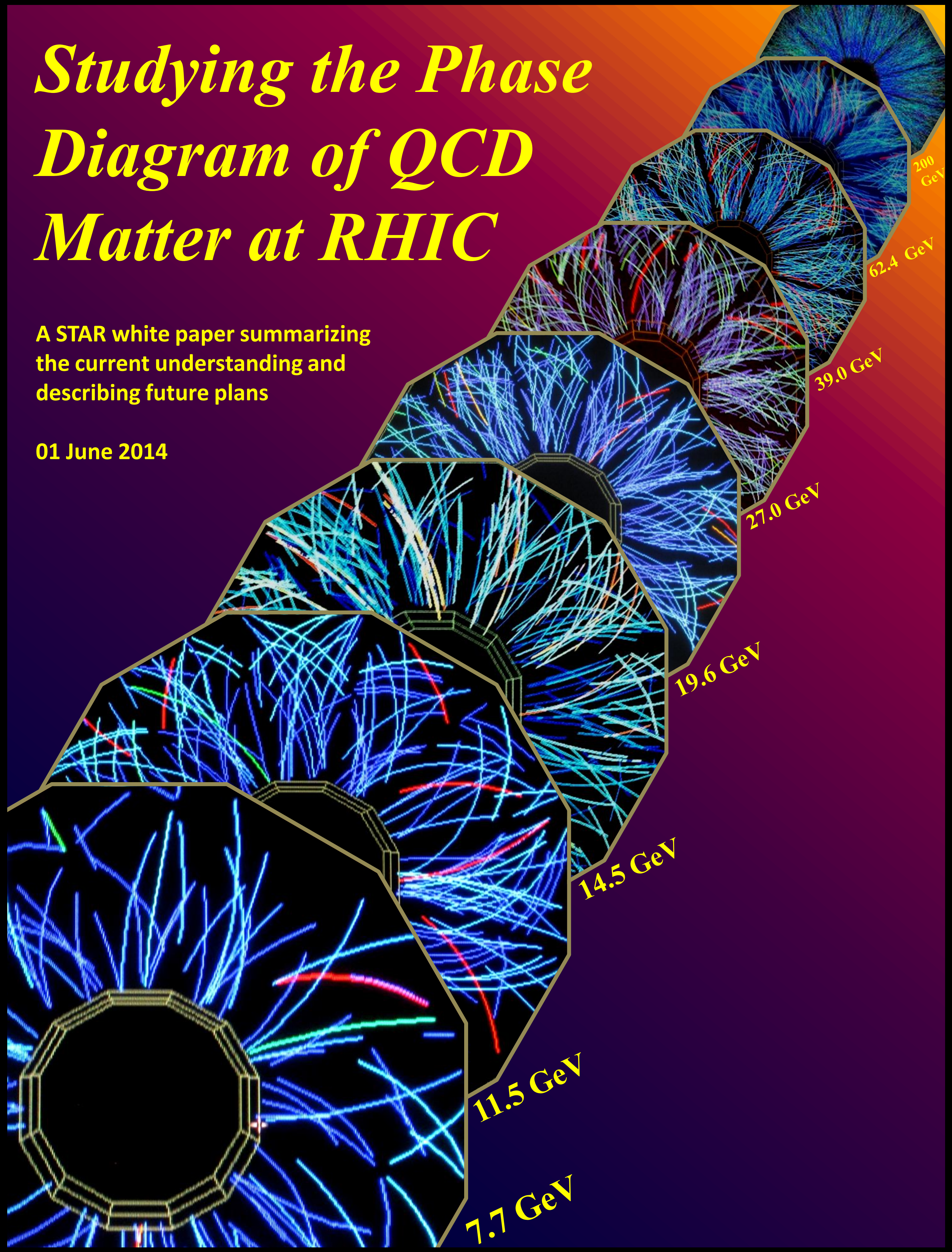

https://drupal.star.bnl.gov/STAR/starnotes/public/sn0598

2. Origin of nucleon spin

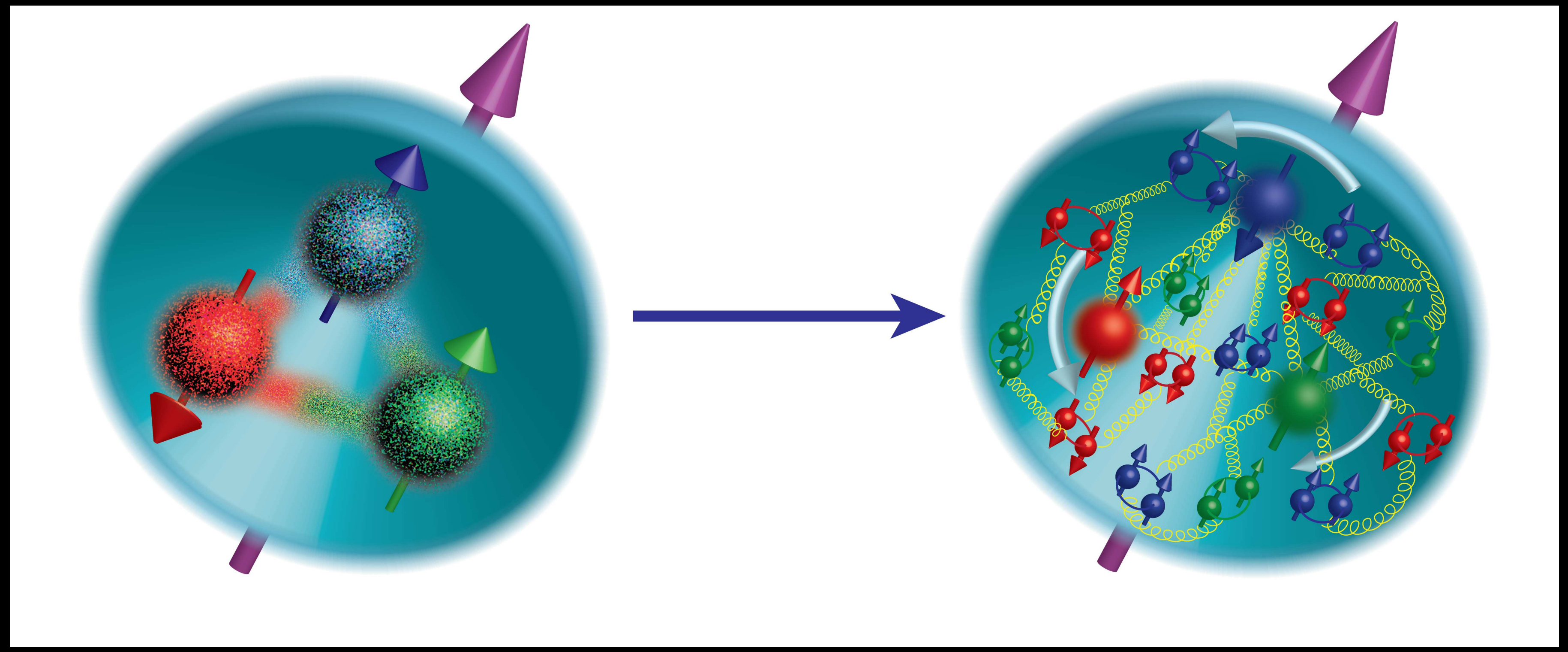

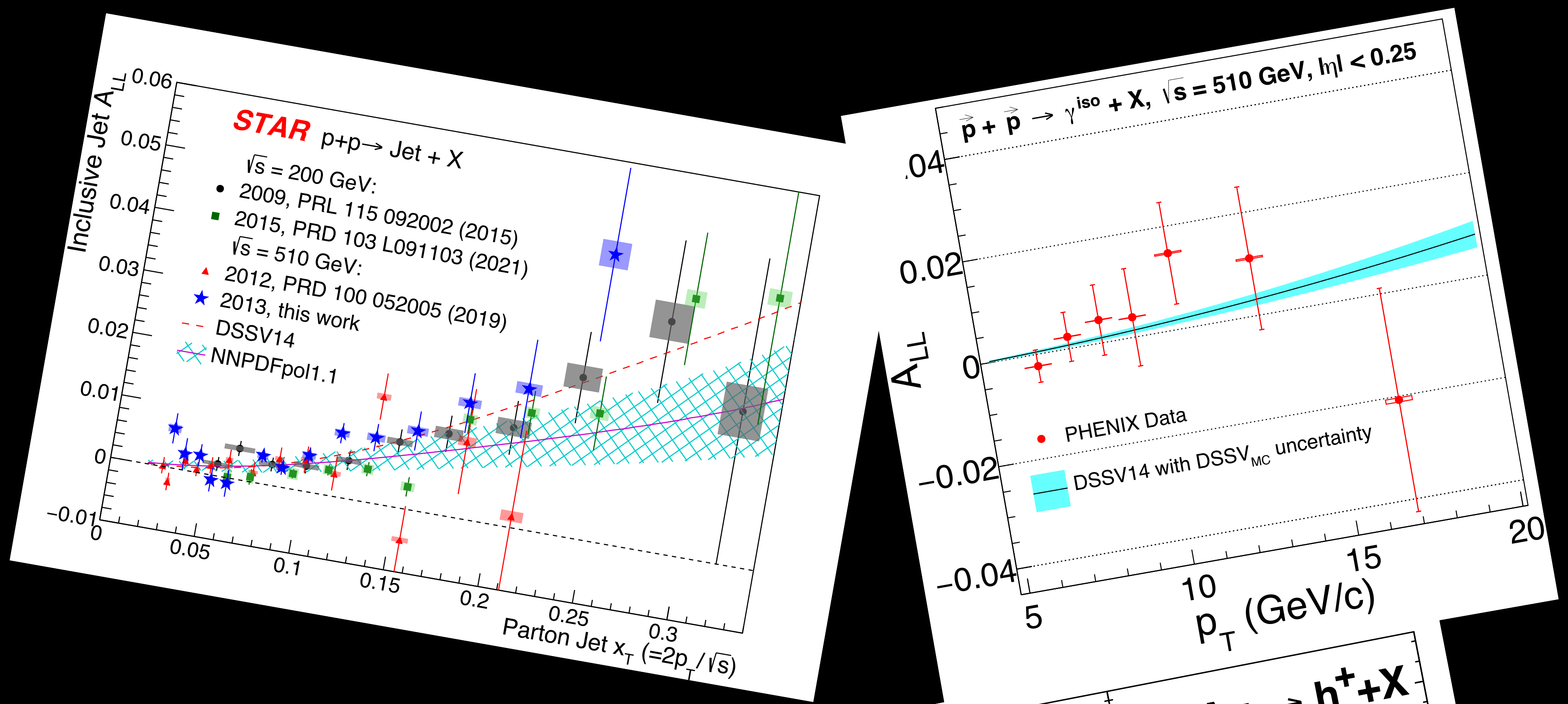

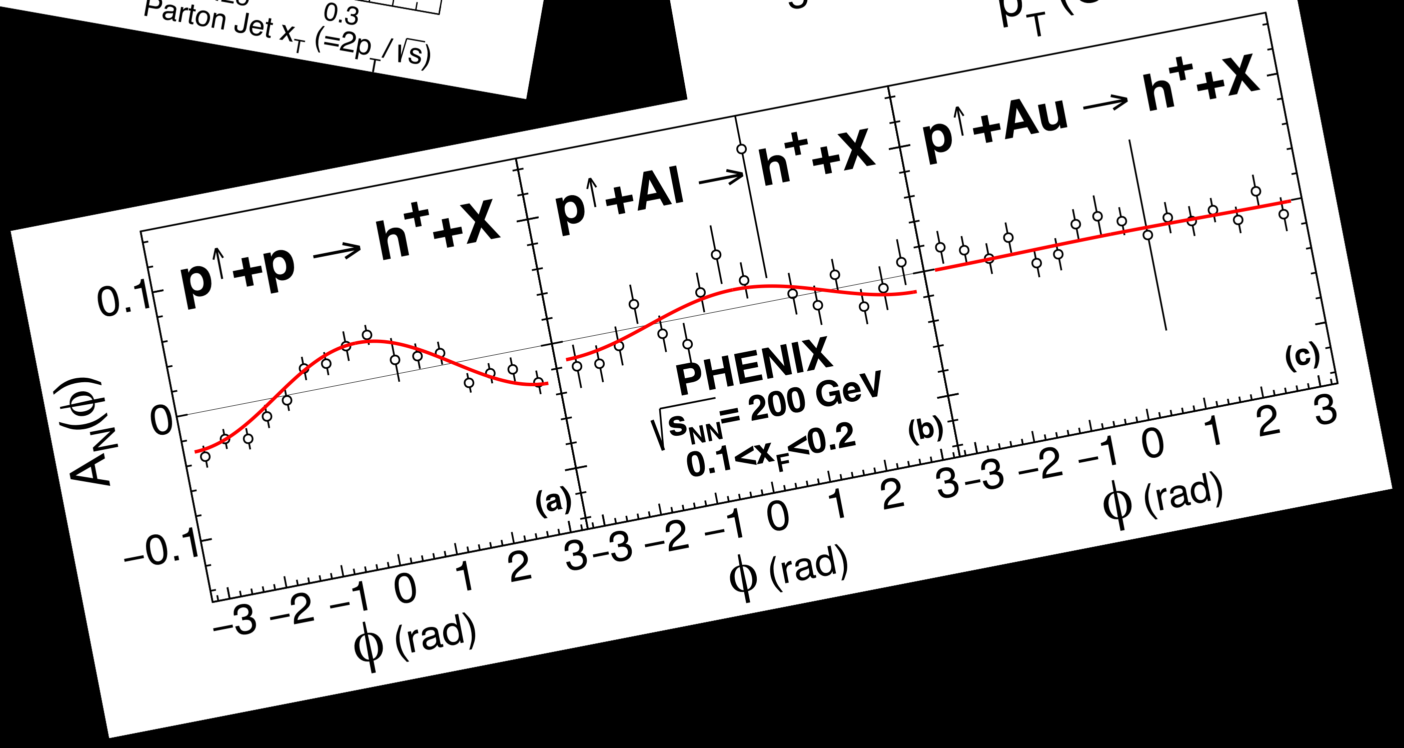

For an introduction and broader ramifications of this field see e.g.
Universe 3(2017)1, 7
Universe 7(2021)9, 330
Universe 8(2022)9, 451

Standard Model of ultrarelativistic heavy ion collisions:

① *All hard hadronic process are strongly quenched*

② *All soft particles emerge from the common flow field*

Successful Operation of STAR in Years 2020-21

RHIC Beam Energy Scan II and p+p 510 run with fully installed forward upgrade

Run 20 and 21 completed successfully: enhanced collision rates due to Low Energy RHIC Electron Cooling system, smooth & desired performance of BES-II upgrades (iTPC, eTOF, EPD)

STAR: Phys.Rev.C 96 (2017) 4, 044904

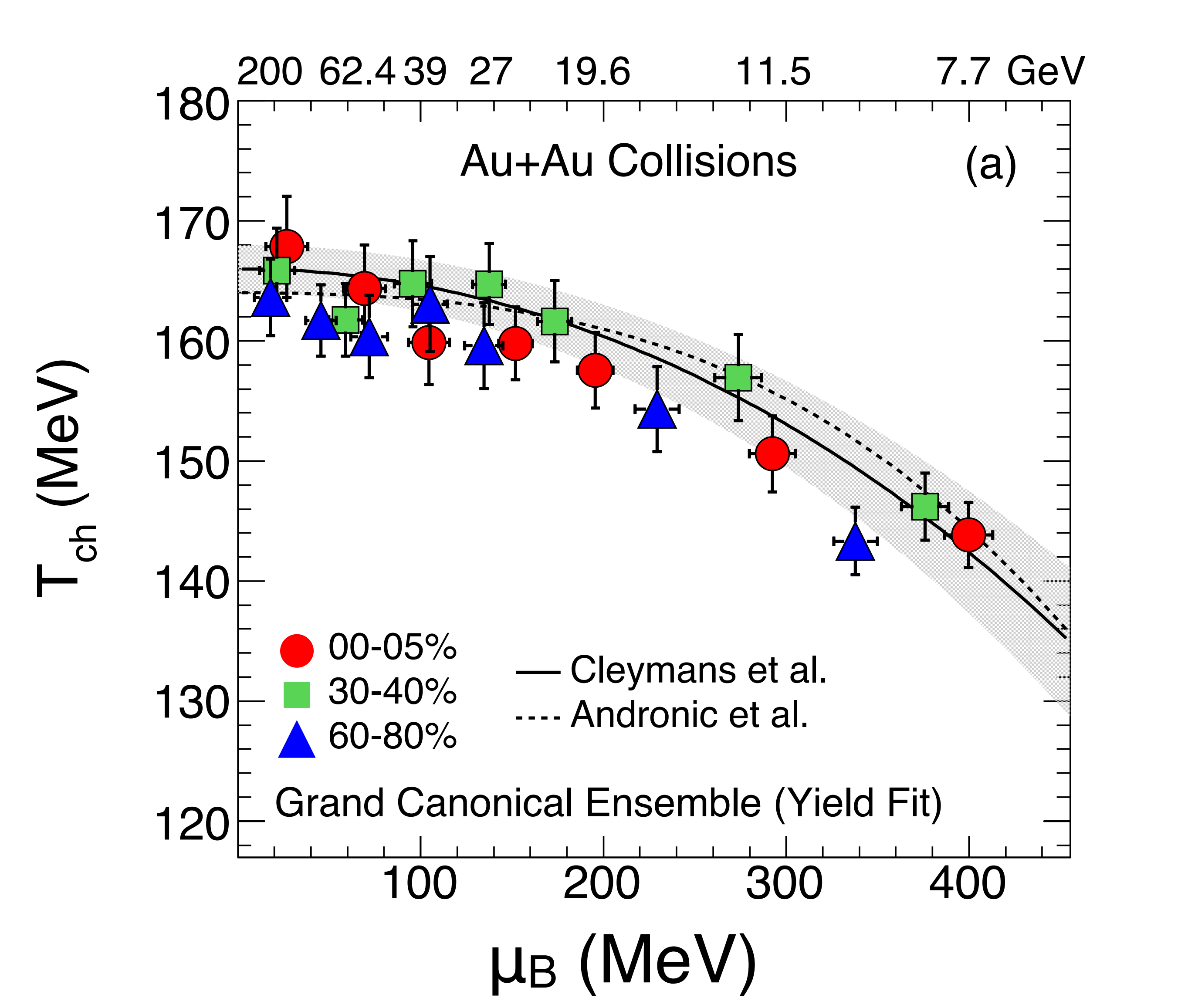

Accessing phase diagram of QCD by varying $\sqrt{s_{NN}}$ changes T and μ_B

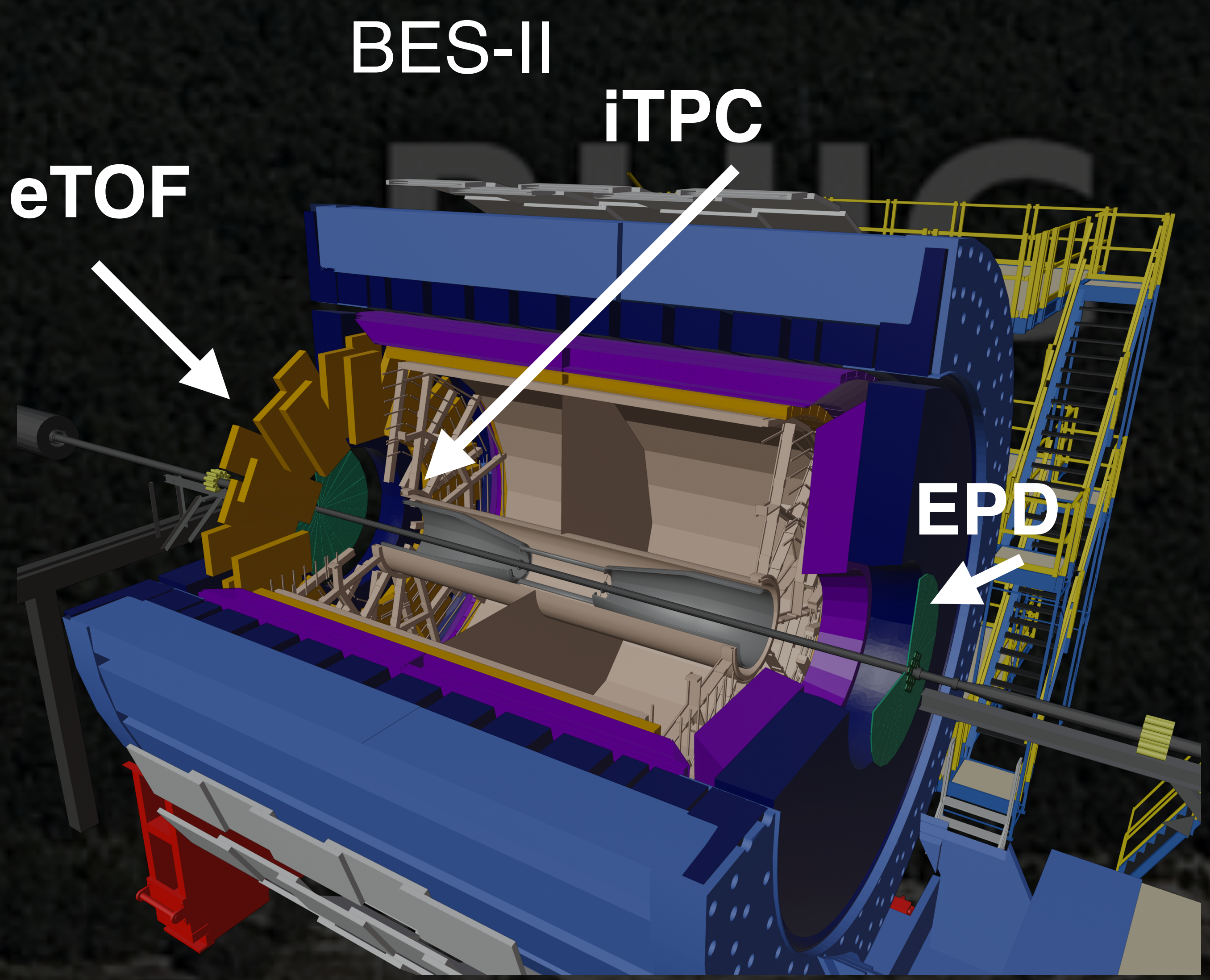

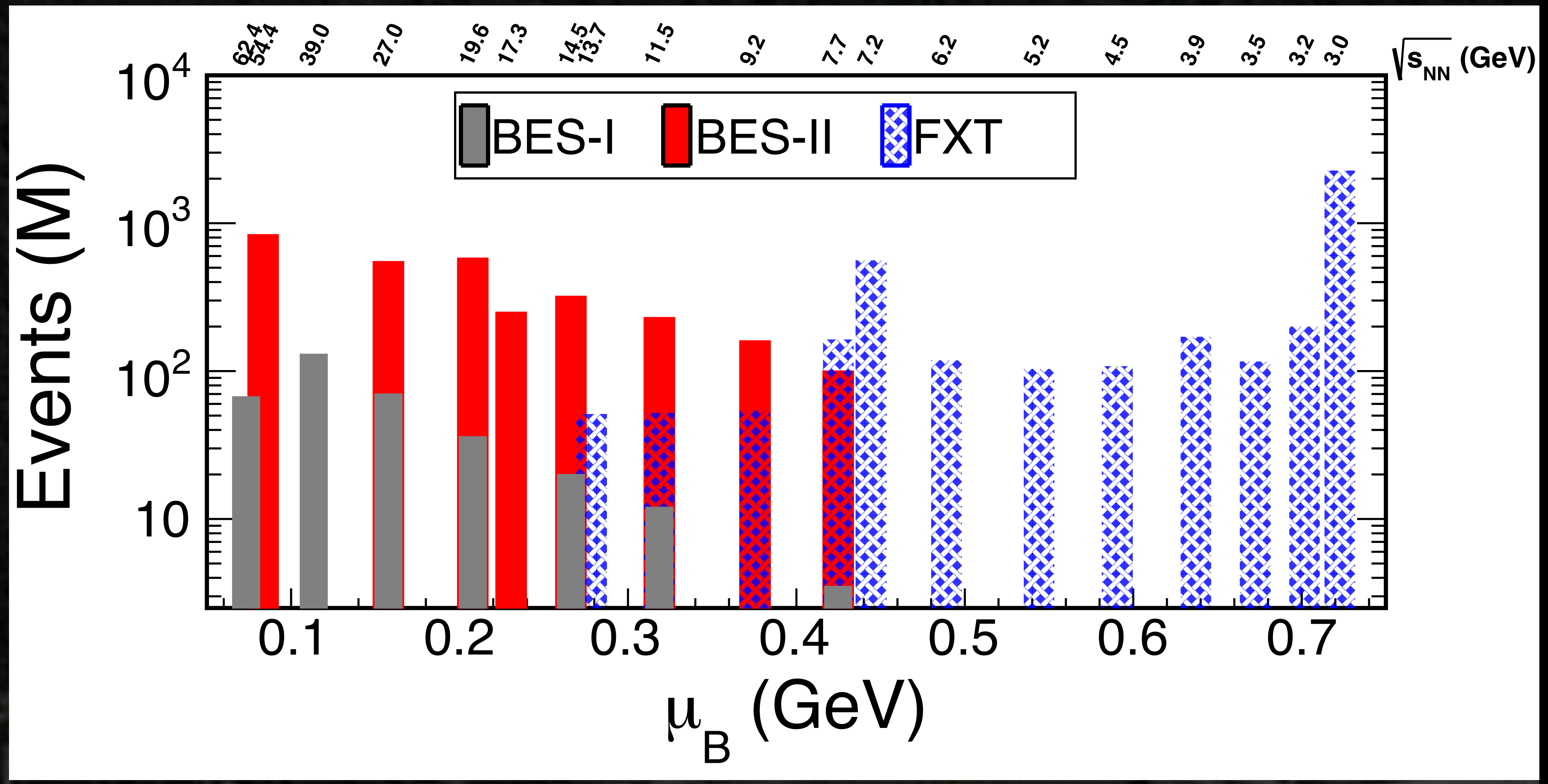

7 energies between 7.7 - 27 GeV (collider mode)
12 energies between 3.0 - 13.7 GeV (FXT mode)

Search for the QCD critical point using cumulants

STAR: Phys.Rev.Lett. 126 (2021) 092301

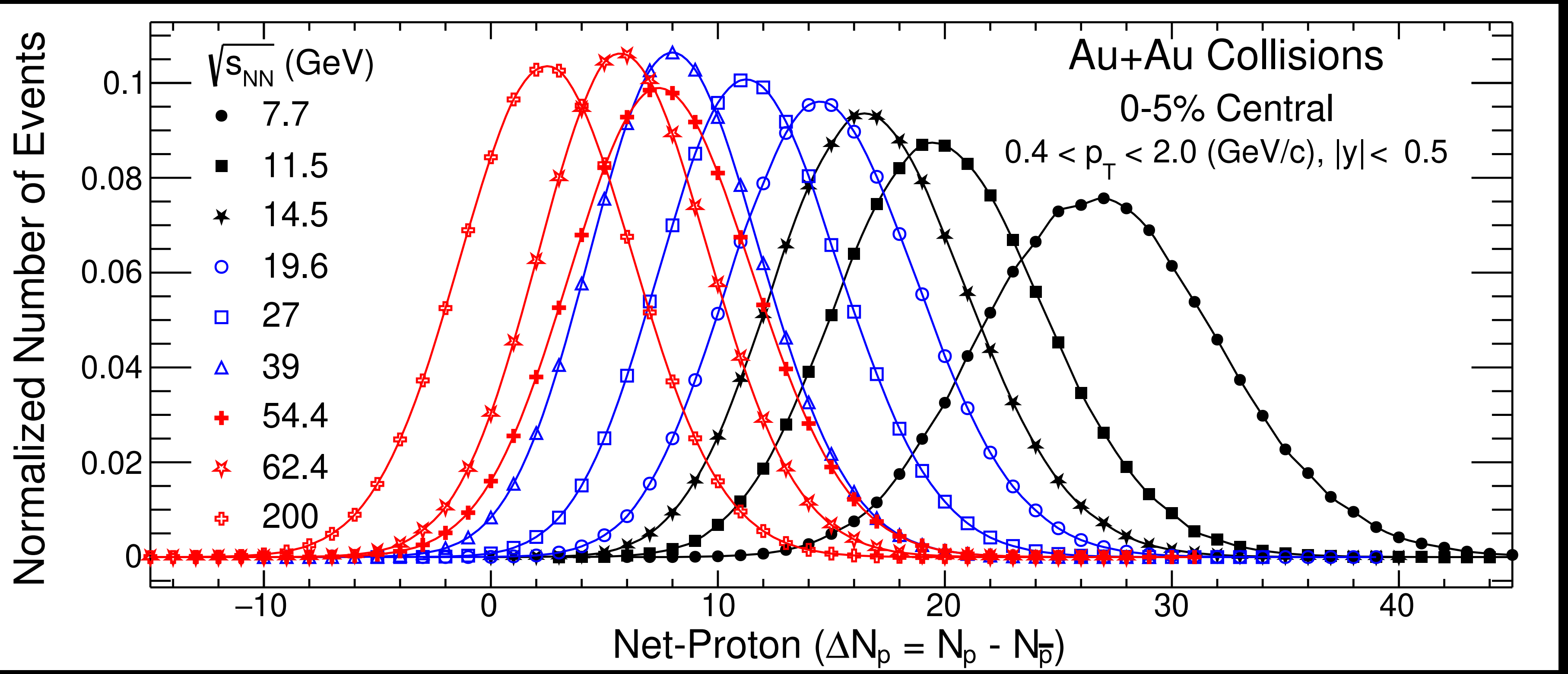

STAR: 2207.09837 [nucl-ex]

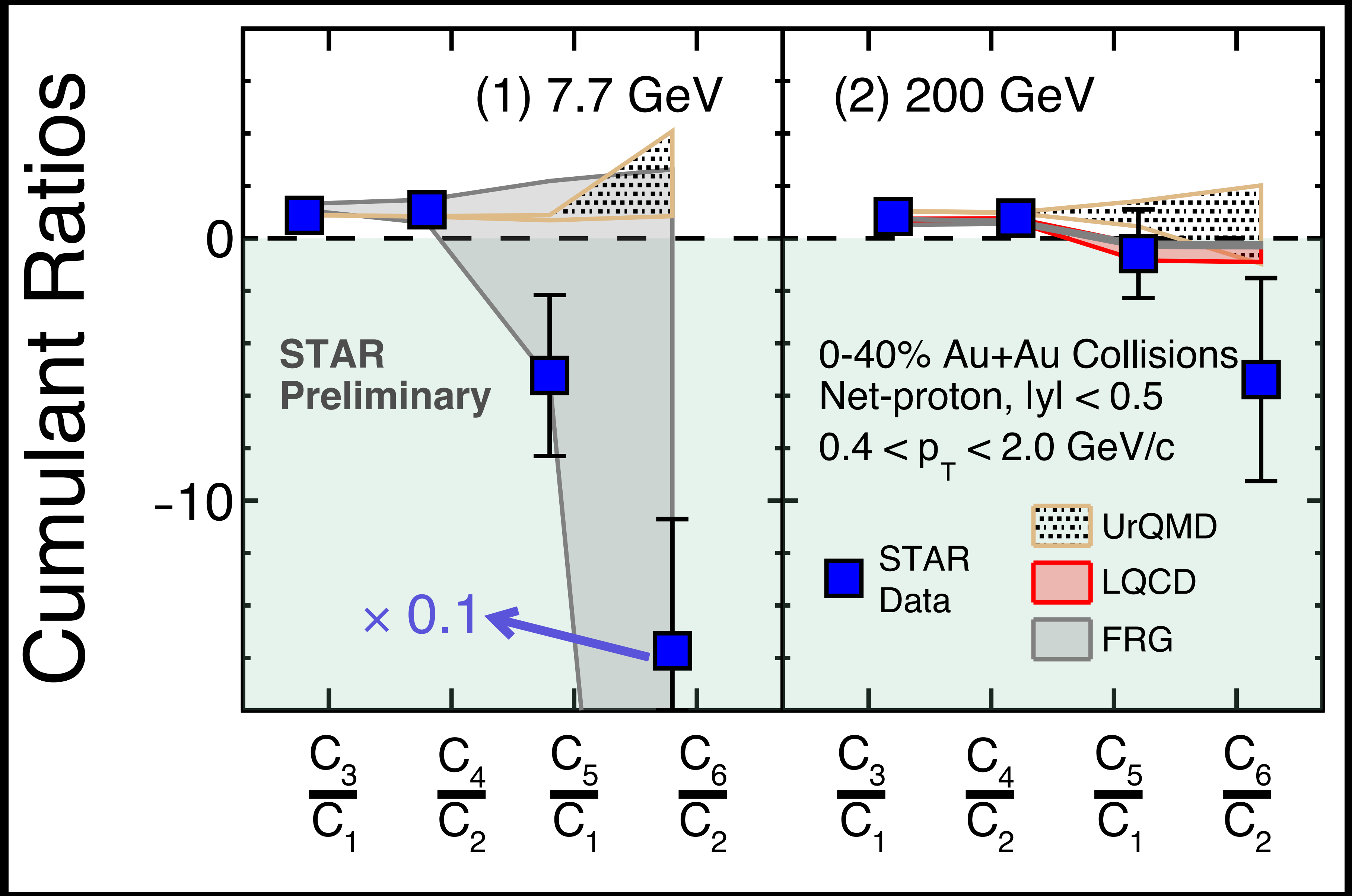

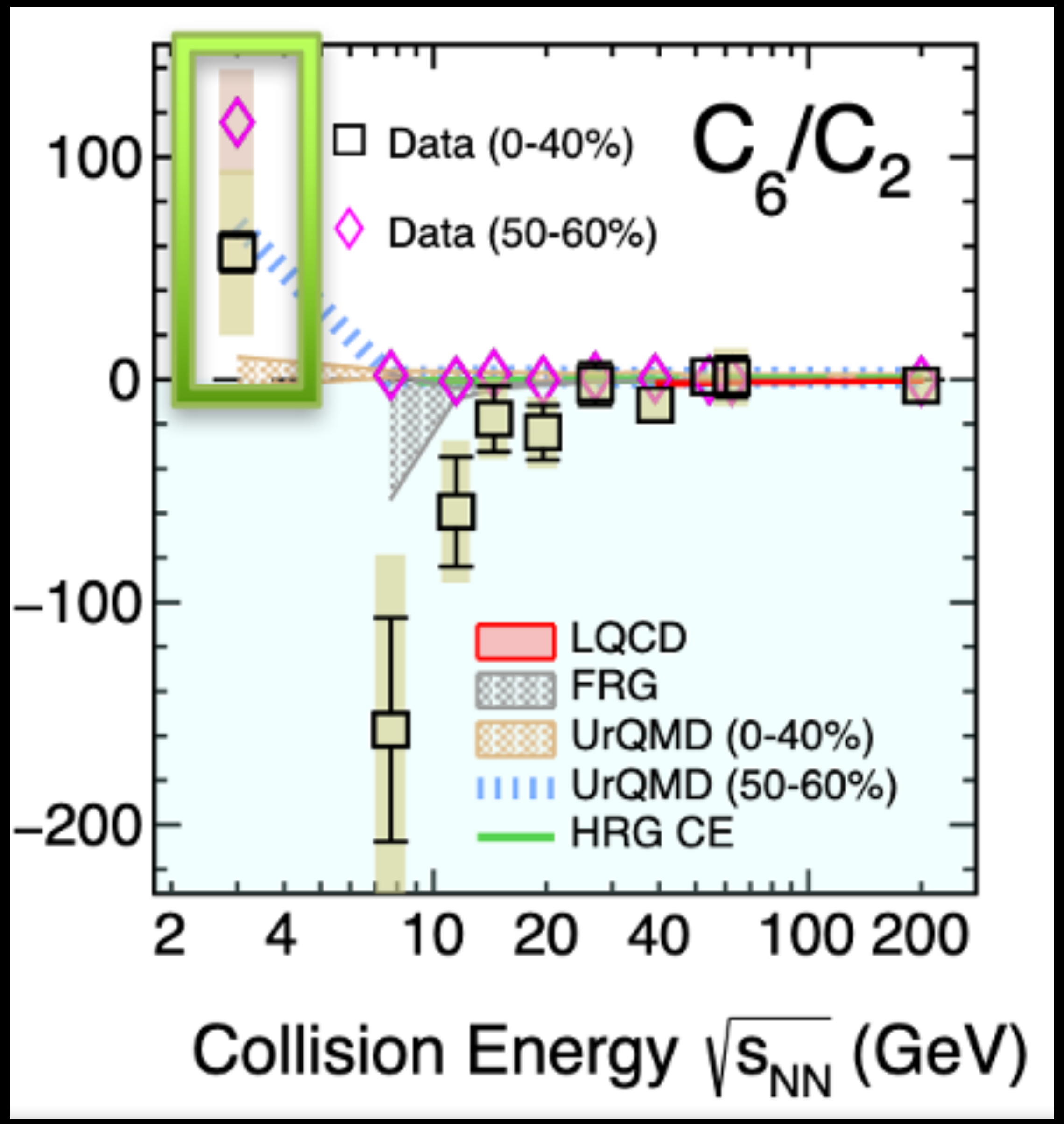

Connect to Theory:

Correlation length ξ

Susceptibility χ_q

$$C_2 \sim \xi^2 \quad C_4 \sim \xi^7$$

$$\chi_q^{(n)} = \frac{\partial^n (p/T^4)}{\partial(\mu_q/T)^n}$$

$$q = B, Q, S$$

$$C_n = VT^3 \chi_q^{(n)}$$

$$\frac{\chi_q^{(4)}}{\chi_q^{(2)}} = \kappa\sigma^2 = \frac{C_{4,q}}{C_{2,q}}$$

$$\frac{\chi_q^{(3)}}{\chi_q^{(2)}} = S\sigma = \frac{C_{3,q}}{C_{2,q}}$$

Sensitive to:

(1) Nature of transition
(2) Critical point
(3) Freeze-out
(4) Thermalization
(5) Initial EM fields

M.A.Stephanov, PRL 107 (2011), 052301

$$C_3/C_1 > C_4/C_2 > C_5/C_1 > C_6/C_2$$

Susceptibility ratio (cumulants) ordering expected from QCD thermodynamics
Phys. Rev. D 101, 074502 (2020)

In 40% most central collisions sign change at the lowest $\sqrt{s_{NN}}$ (Significance ~ 1.7σ_{tot})
Consistent with LQCD
Absent in more peripheral data

N.B. Cumulants C_n are additive combination of central moments μ_n.
The n-th-order cumulant of the sum of independent random variables equals the sum of their n-th-order cumulants.

Search for the chiral crossover transition

Cumulant ratios C_5/C_1 and C_6/C_2 of net-proton measured with p+p, Au+Au and high statistics isobar data at $\sqrt{s_{NN}}$ = 200 GeV show decreasing trend with multiplicity, approaching LQCD predictions

STAR: Phys. Rev. Lett. 127, 262301

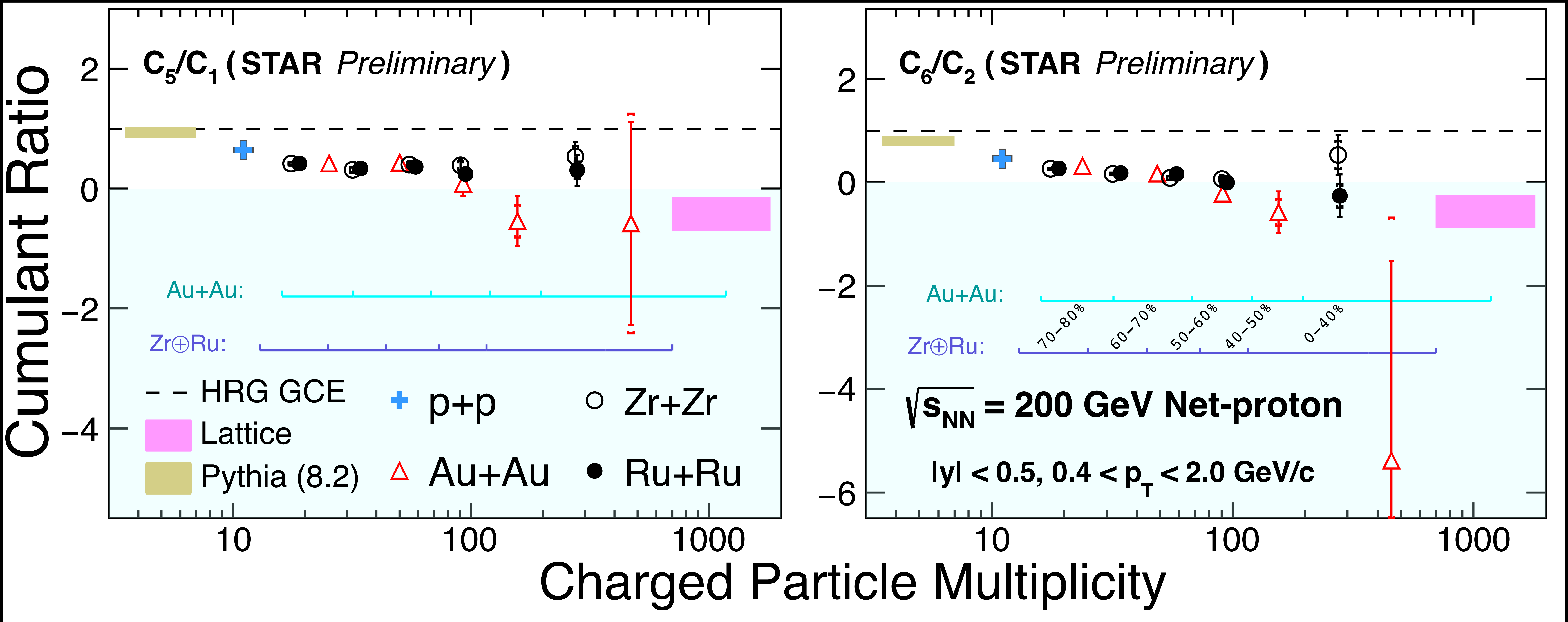

High multiplicity measurements are consistent with results from lattice QCD that predicts crossover at μ_B =0

Non-trivial interplay between hydrodynamics and magnetic field

Experiment: STAR, Nature 548, 34–35 (03 August 2017)

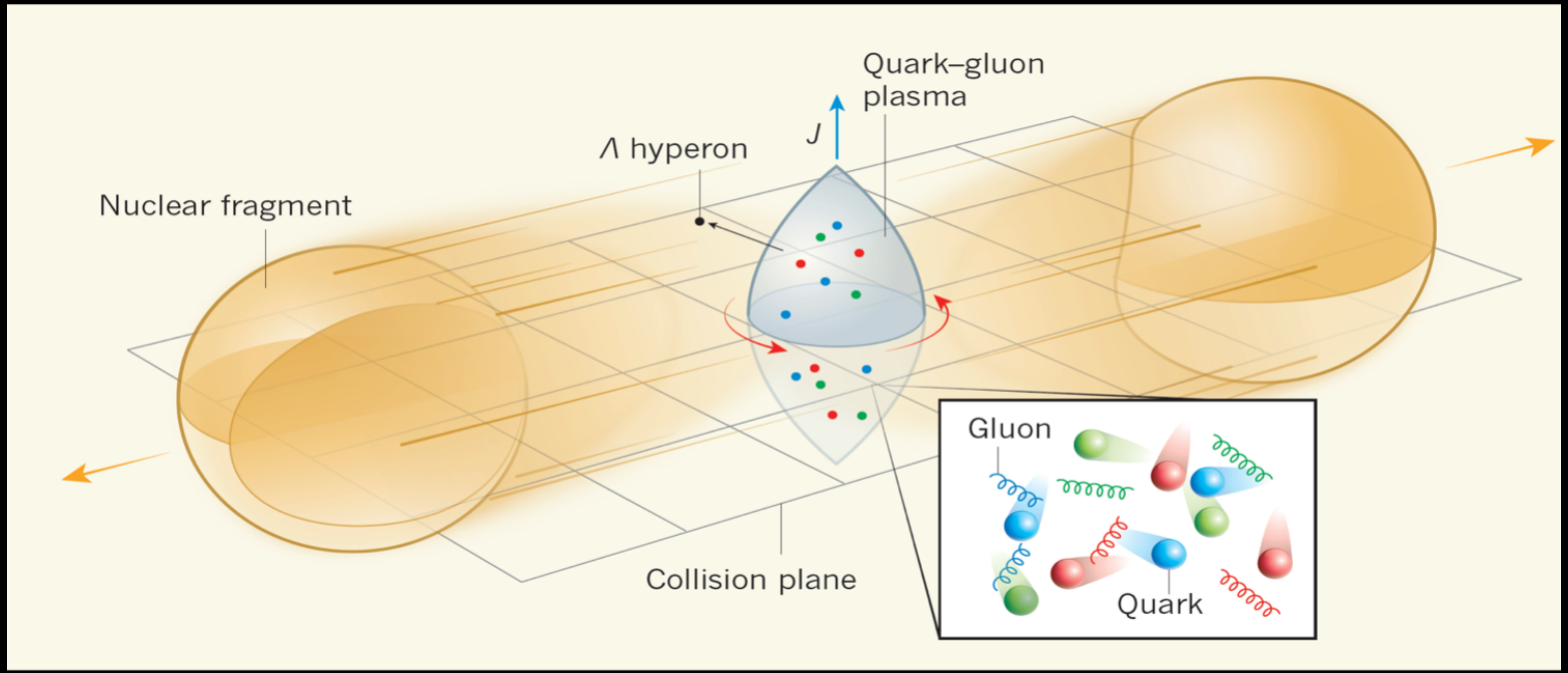

Theory: Becattini, Lisa, Ann.Rev.Nucl.Part.Sci. 70 (2020) 395

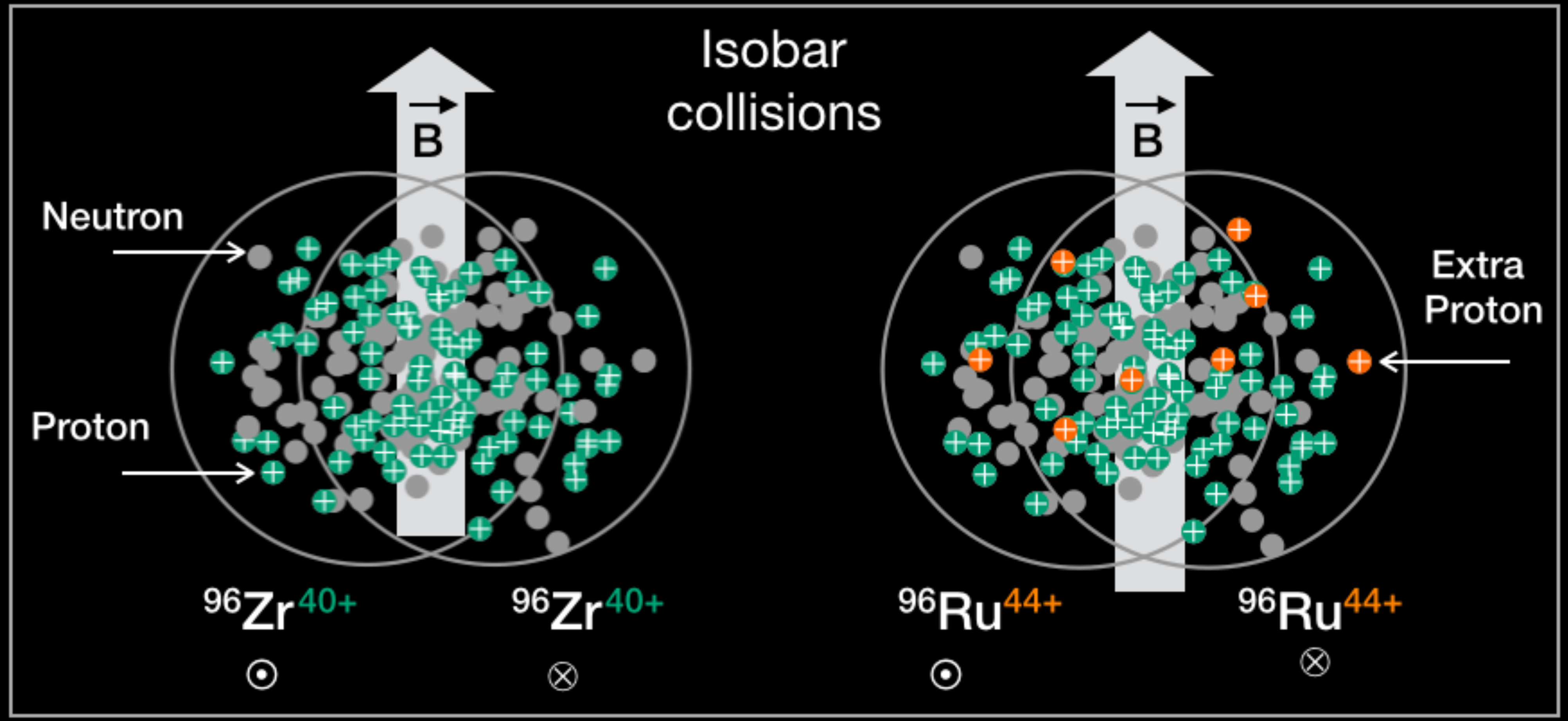

B-field square is 10-15% larger in Ru+Ru than Zr+Zr

- ★ Total angular momentum in non-central heavy ion collisions: $J \sim 10^5\,\hbar \approx N_{part} \times (\sqrt{s_{NN}}/2) \times b)$ (Carruthers 1984)
- ★ In hydrodynamical picture relevant quantity is <u>vorticity</u> $\vec{\omega} = \frac{1}{2}\vec{\nabla} \times \vec{v} \approx \frac{1}{2}\frac{\partial v_z}{\partial x}$
- ★ Fine-scale vorticity at the "point" cell is reflected in the spin of emitted particles
- ★ Λ spin polarization $P = \langle \vec{S} \rangle / |\vec{S}|$, $\langle \vec{S} \rangle = \frac{1}{4}\vec{\omega}_{cell}$, $\Lambda - \bar{\Lambda}$ splitting due to strong magnetic fields
- ★ Biot-Savarat $B_\perp = \gamma Z e \frac{b}{R^3} = \frac{\sqrt{s_{NN}}}{2m_N} Z e \frac{b}{R^3}$, $\gamma = 100,\ Z = 79,\ b = R_A = 7fm \Rightarrow eB = 10^{18}G$

Global lambda polarization with the isobars

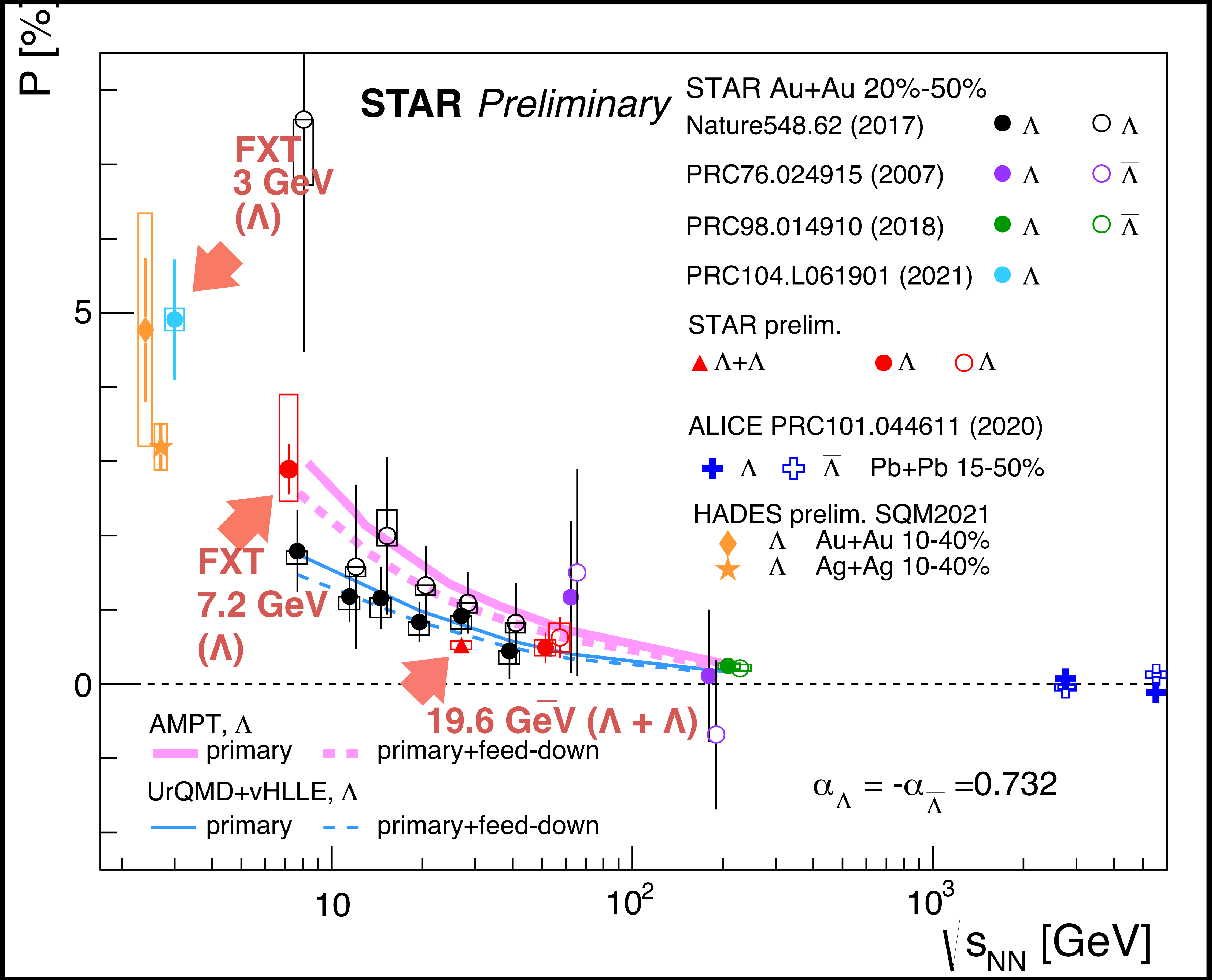

Various predictions tested with high statistics isobar & Au+Au data at $\sqrt{s_{NN}}$= 200 GeV

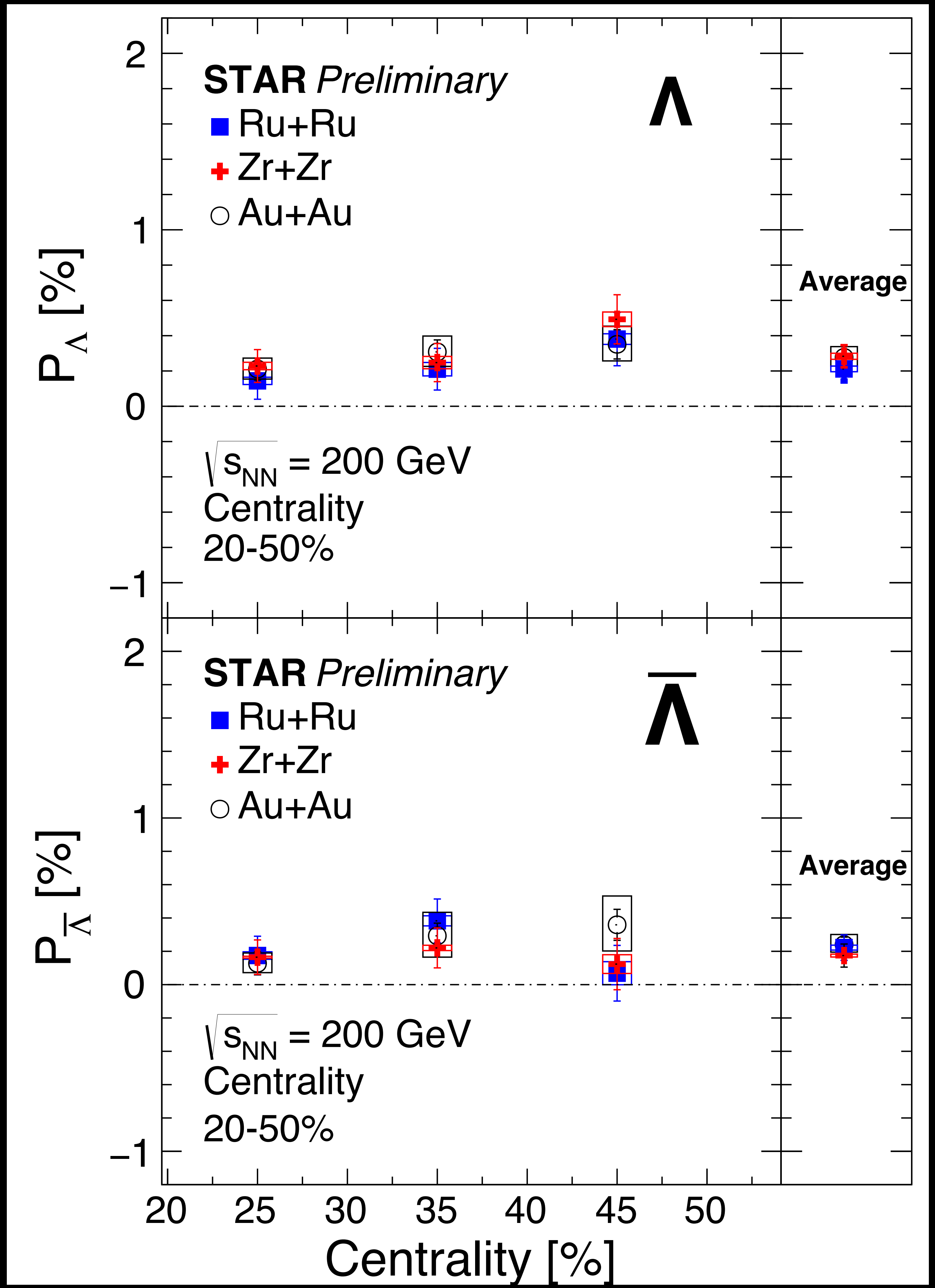

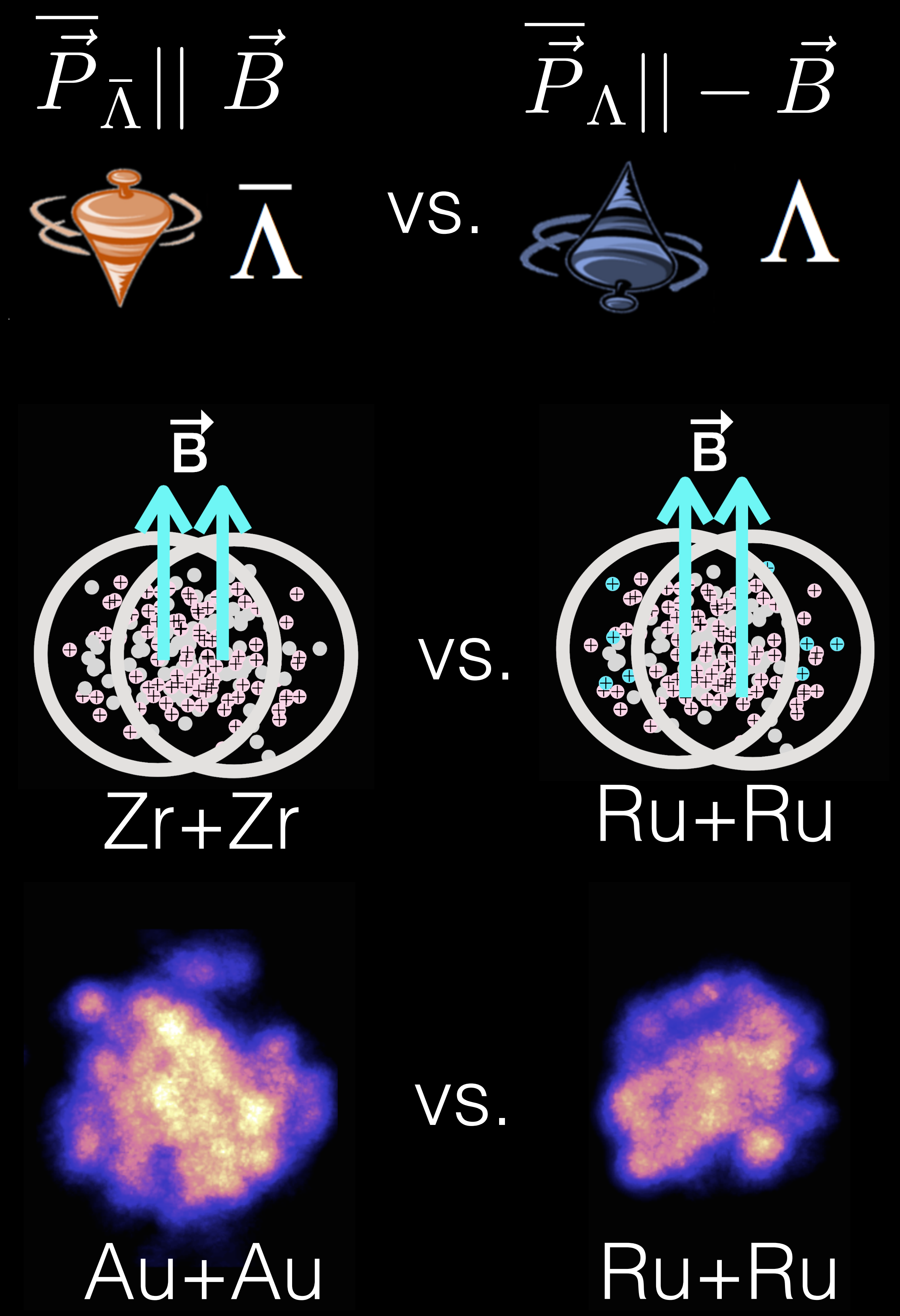

No system dependence at fixed centrality or B-field driven splitting seen in isobar 200 GeV collisions

Perhaps due to nuclear structure difference? (nuclear deformation, neutrons skin) 2208.06941 [nucl-ex]

J/ψ and ϒ in medium at RHIC energies

Quarkonia dissociate in QGP due to color screening of potential between heavy-quarks, Matsui&Satz (1986)

Medium modification of J/ψ studied via R_{AA} in isobar and Au+Au 54.4 GeV, new baseline measurement of R_{pA}

STAR: 2207.06568 [nucl-ex]

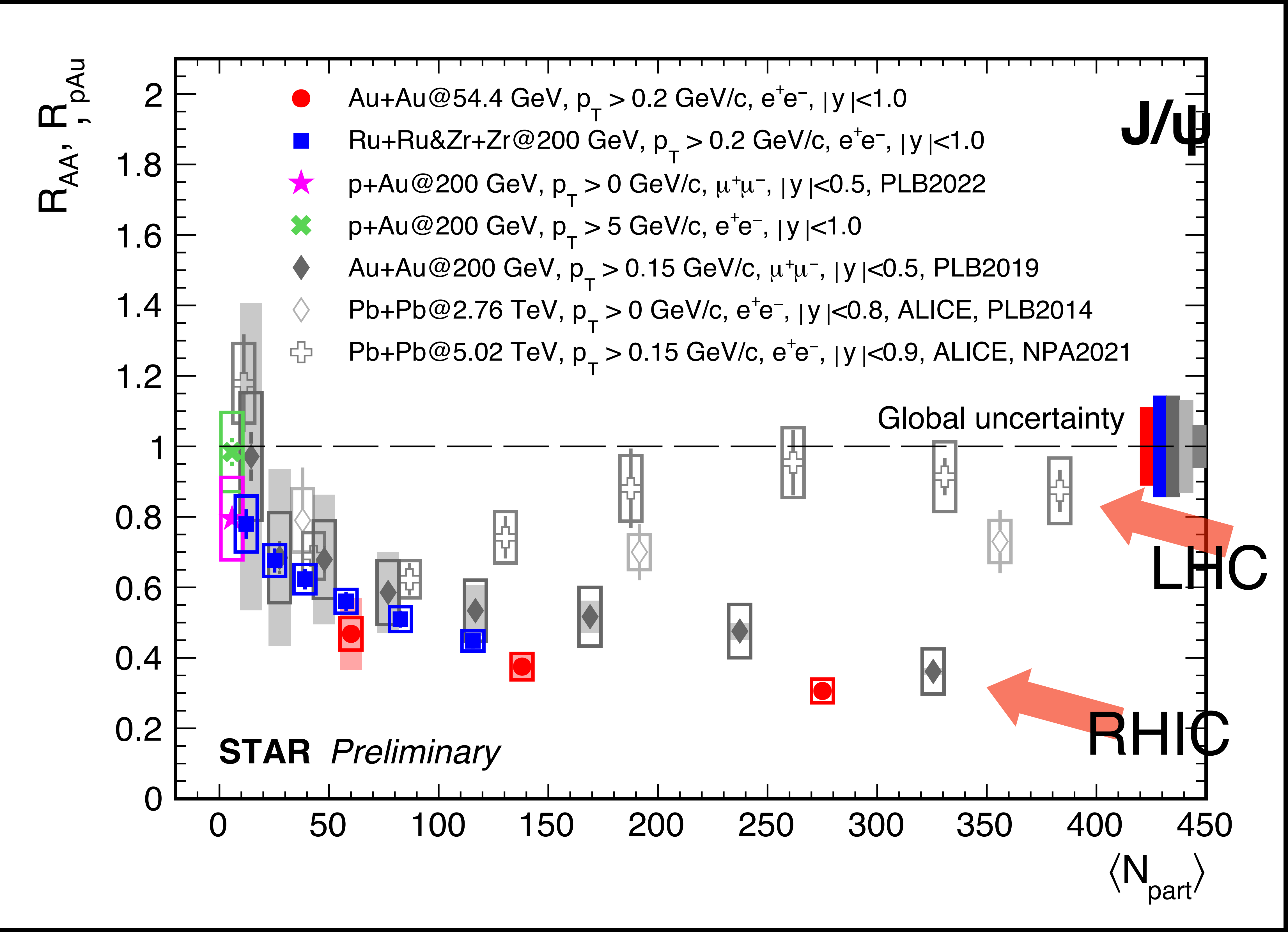

J/ψ suppression at RHIC scales with N_{part}

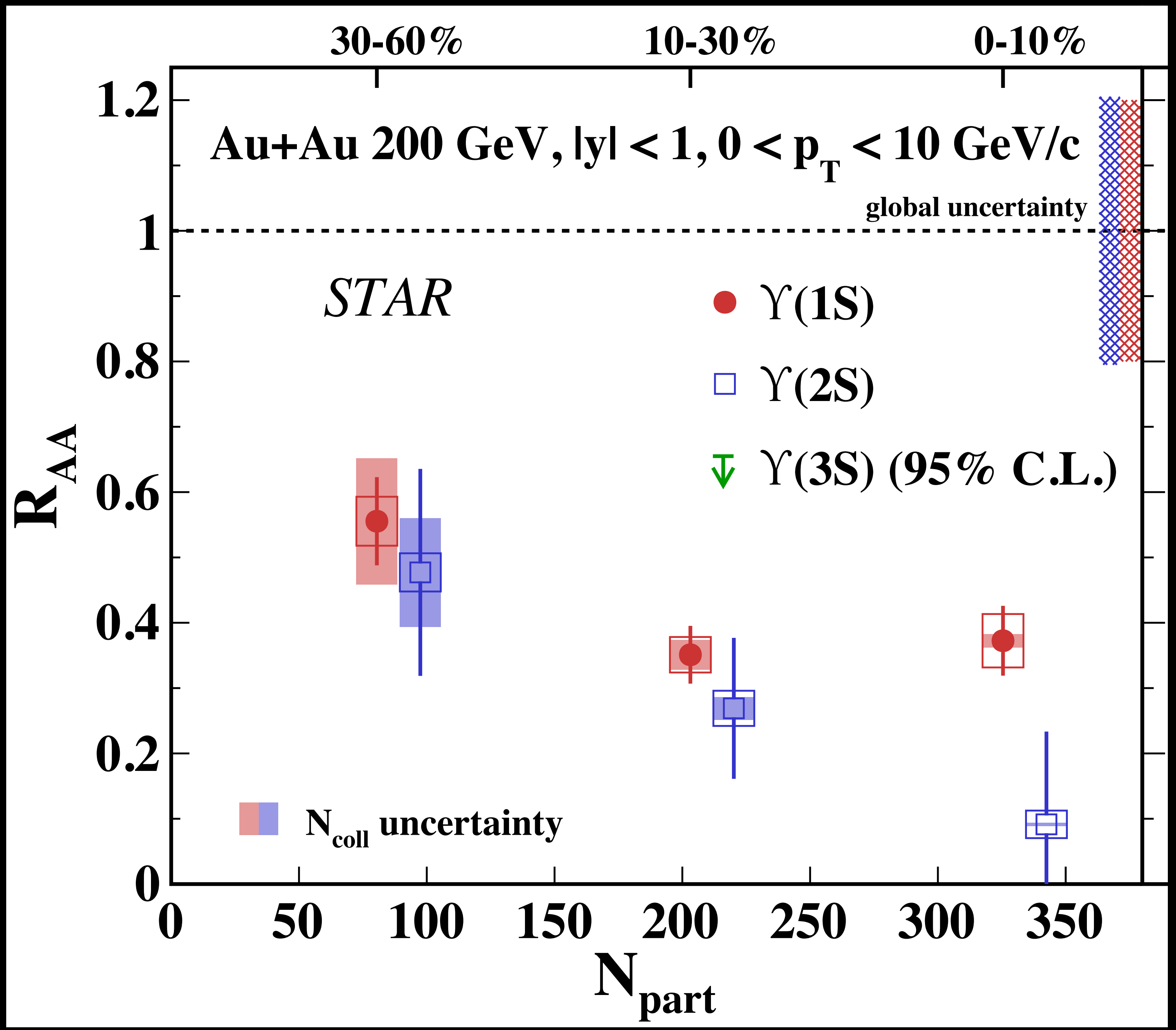

Sequential ϒ suppression

ϒ(1S): R_{AA}@RHIC ≃ R_{AA}@LHC

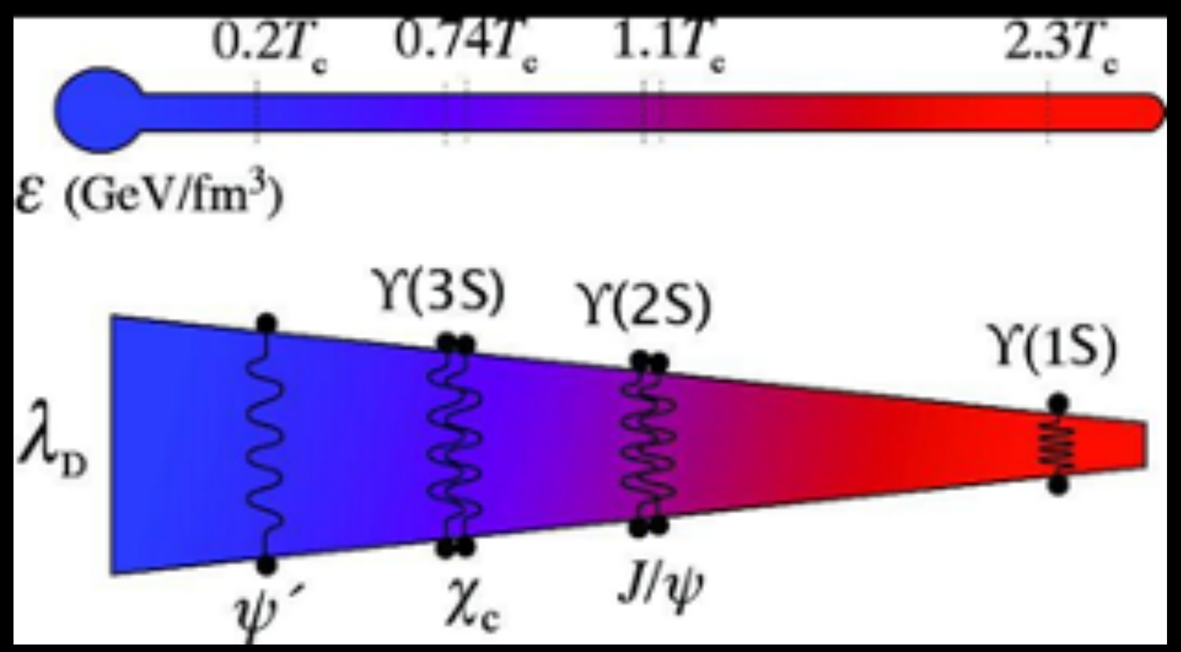

Differences in binding energies lead to a sequential melting of quarkonia with increasing temperature of the QGP

Hadronization of charm quarks in medium

STAR: PRL 124 (2020) 17, 172301

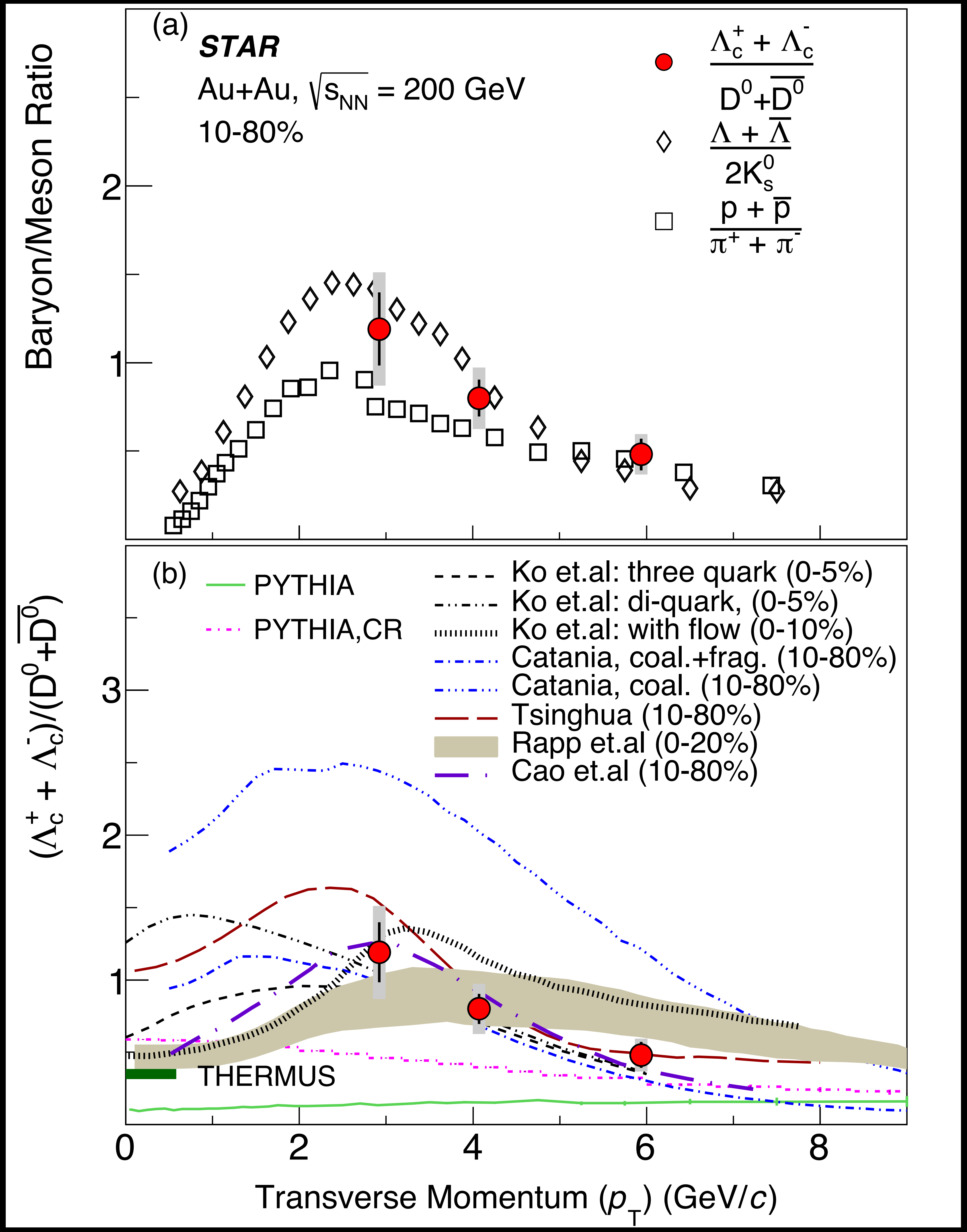

STAR: 2112.08156 [nucl-ex]

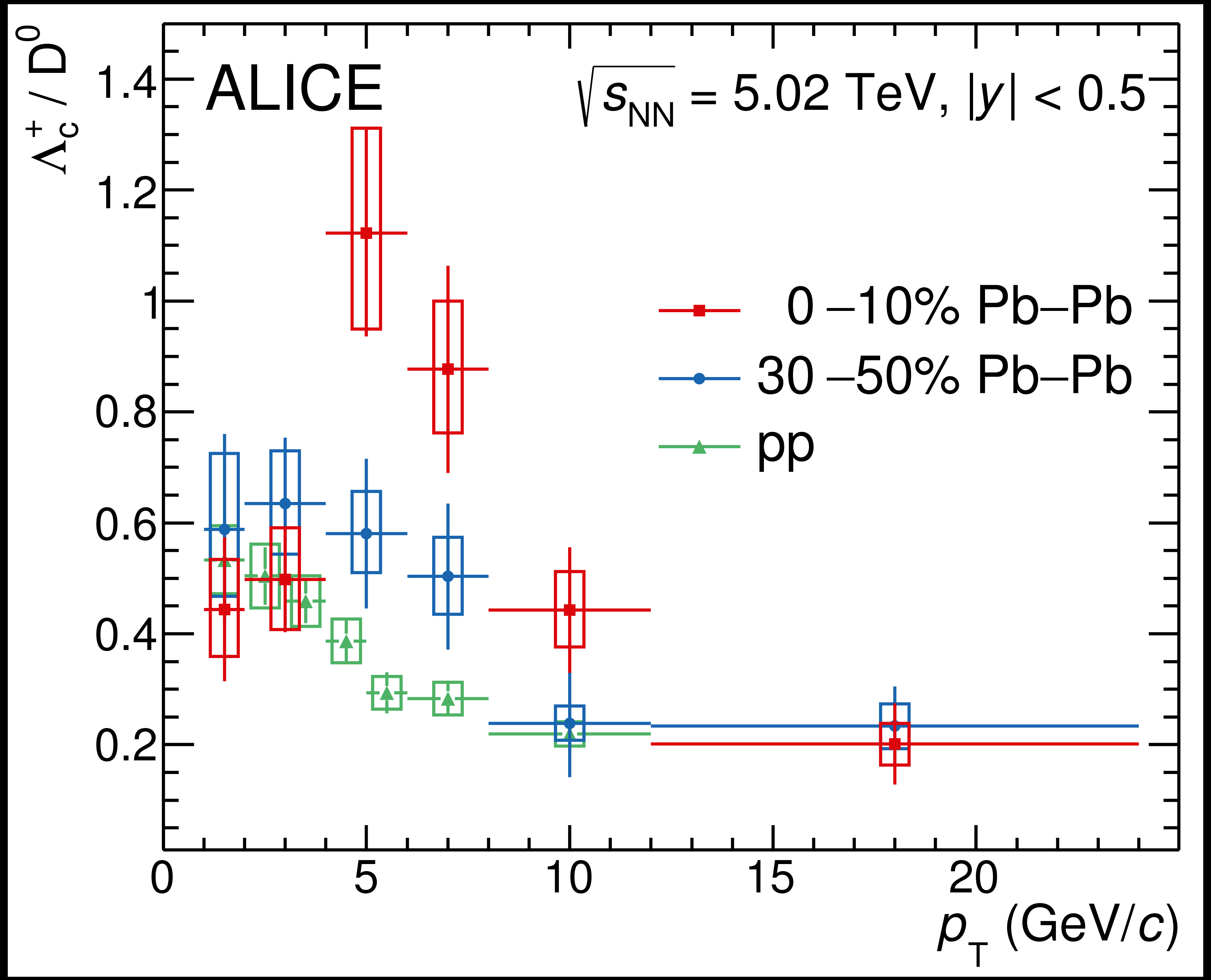

<u>Additional dynamics in QGP:</u>

Λ_c/D^0 enhancement at intermediate p_T relative to pp present from RHIC to LHC

→ similar to light flavor hadrons

→ parton recombination at play also for c quarks

Medium-induced broadening of jets

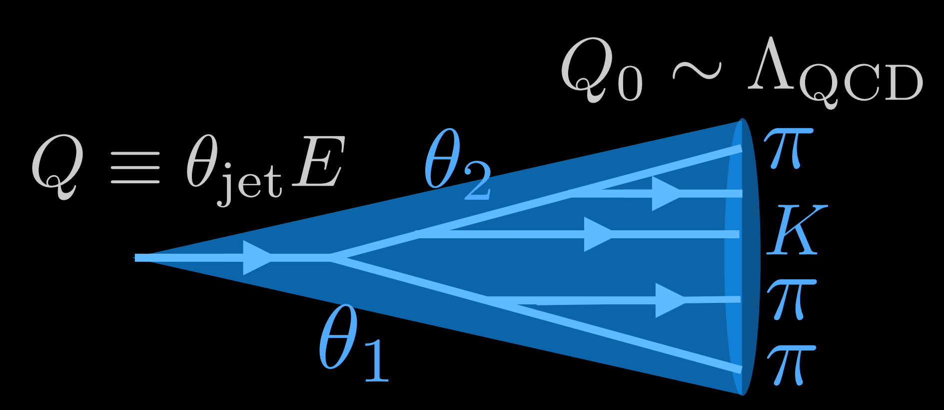

Vacuum shower (p+p)

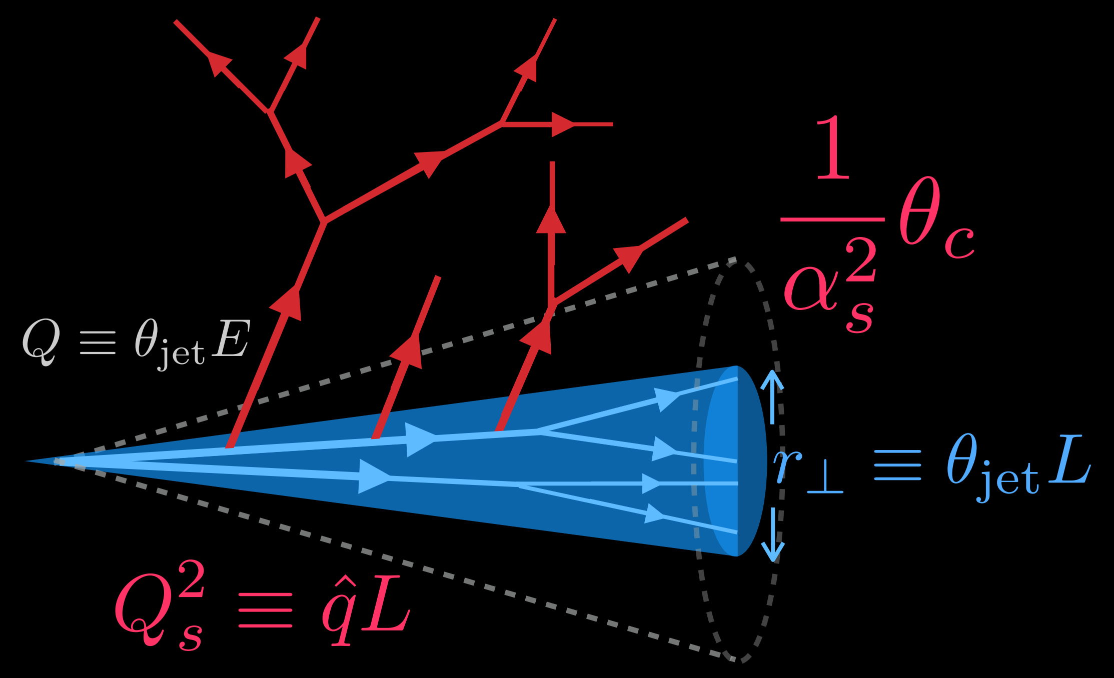

Medium induced gluon radiation (Au+Au)

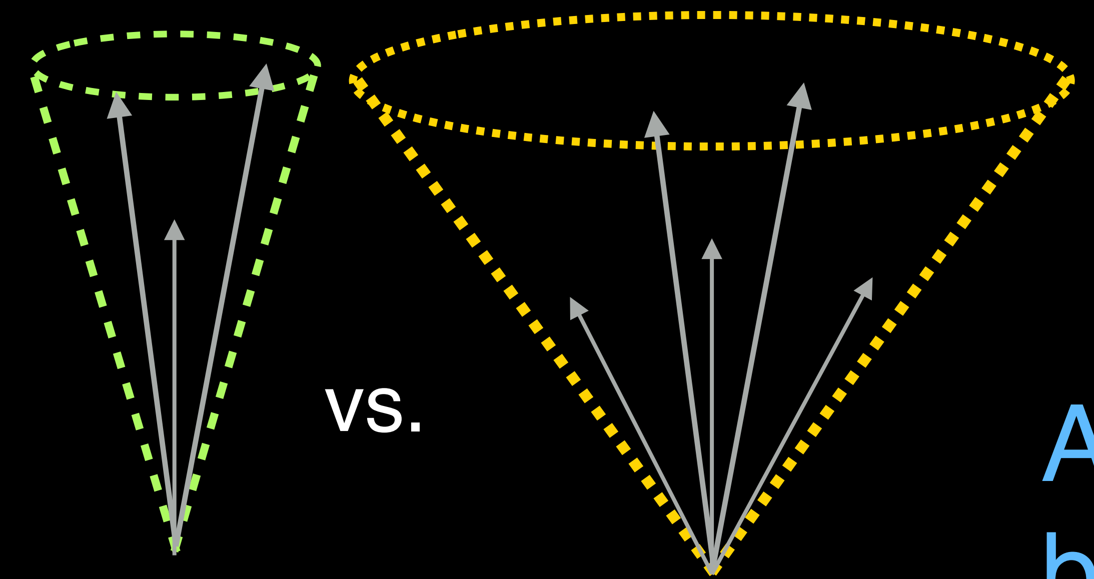

R=0.2 / R=0.5

Ratio of jet spectra for two cone sizes For semi-inclusive π^0/γ+jets is lower in Au+Au than p+p measurements

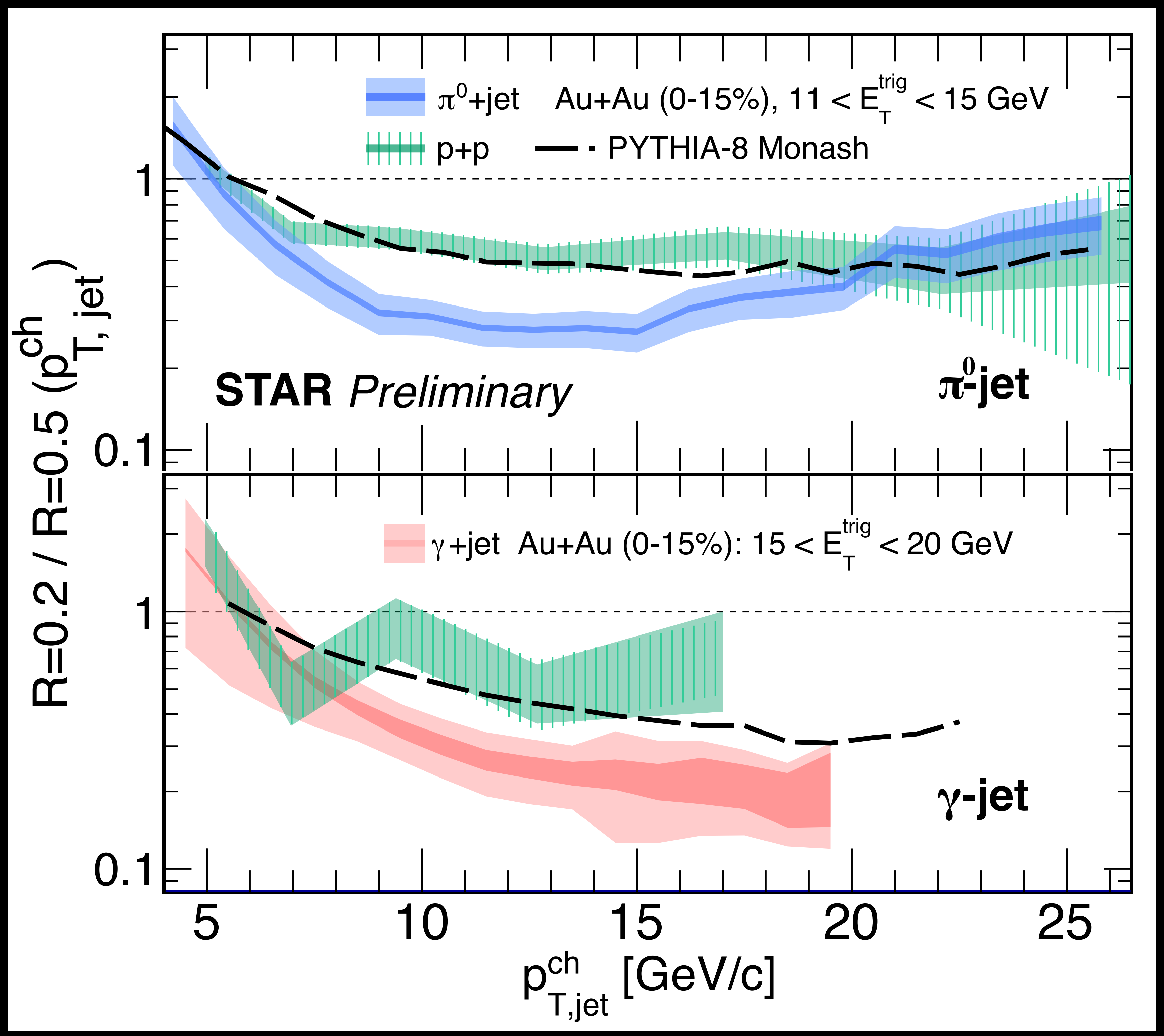

A clear observation of medium-induced broadening of jet-shower at RHIC

Excess yield at large angle for π^0/γ+jet in Au+Au observed compared to p+p PYTHIA baseline

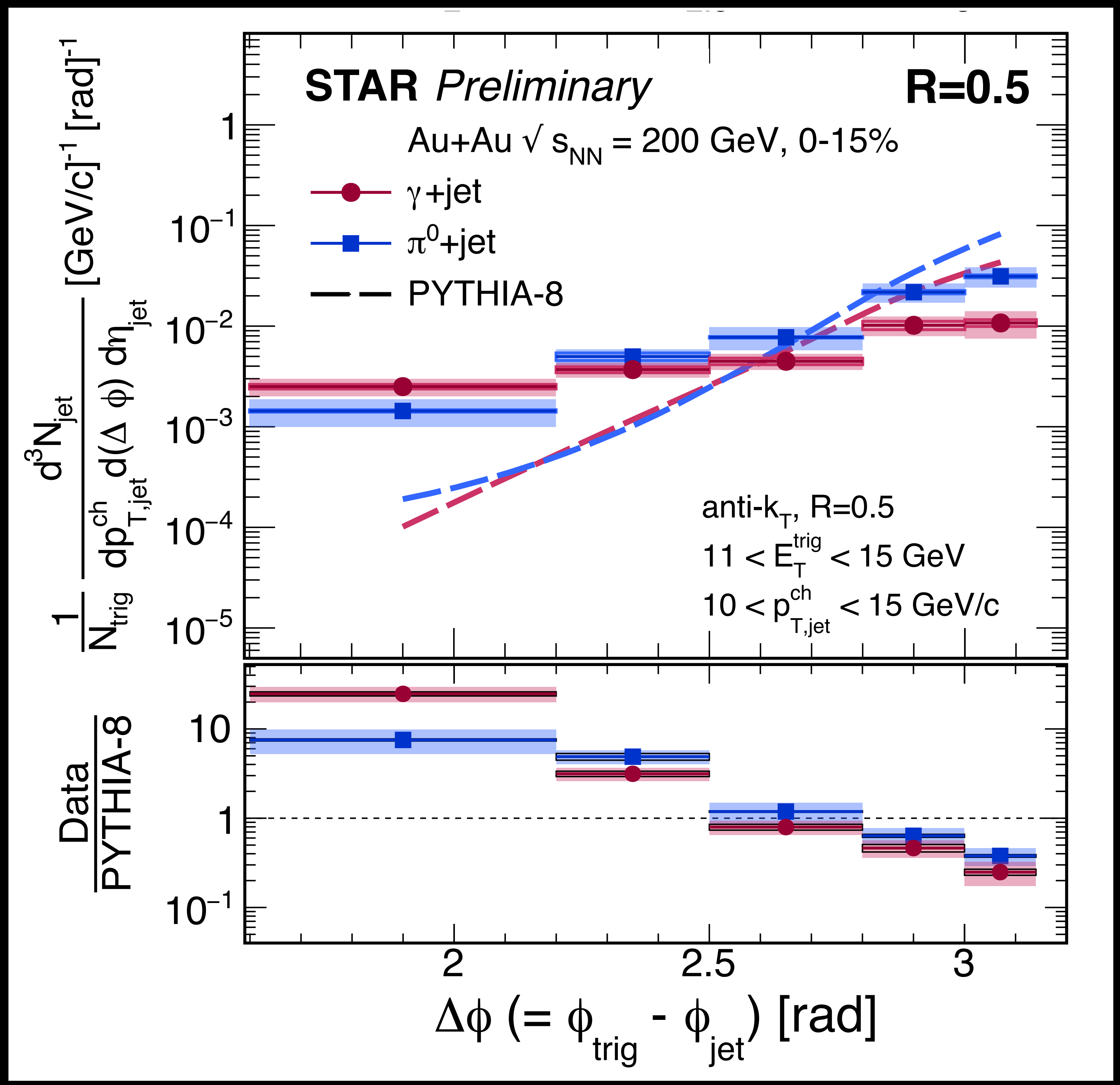

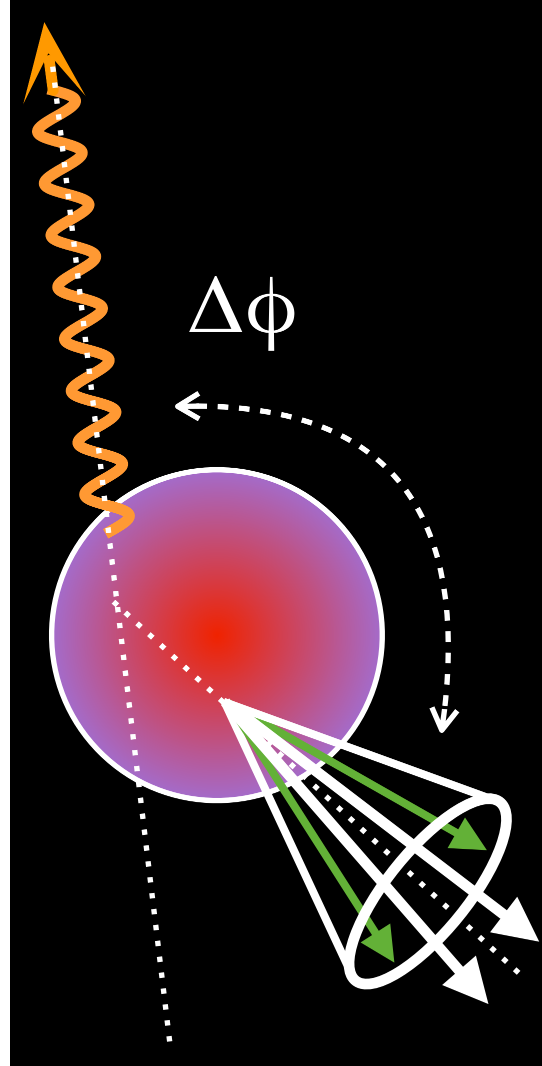

First observation of medium-induced broadening of acoplanarity

Nonprompt direct photon production in Au+Au@$\sqrt{s_{NN}}$=200GeV

PHENIX

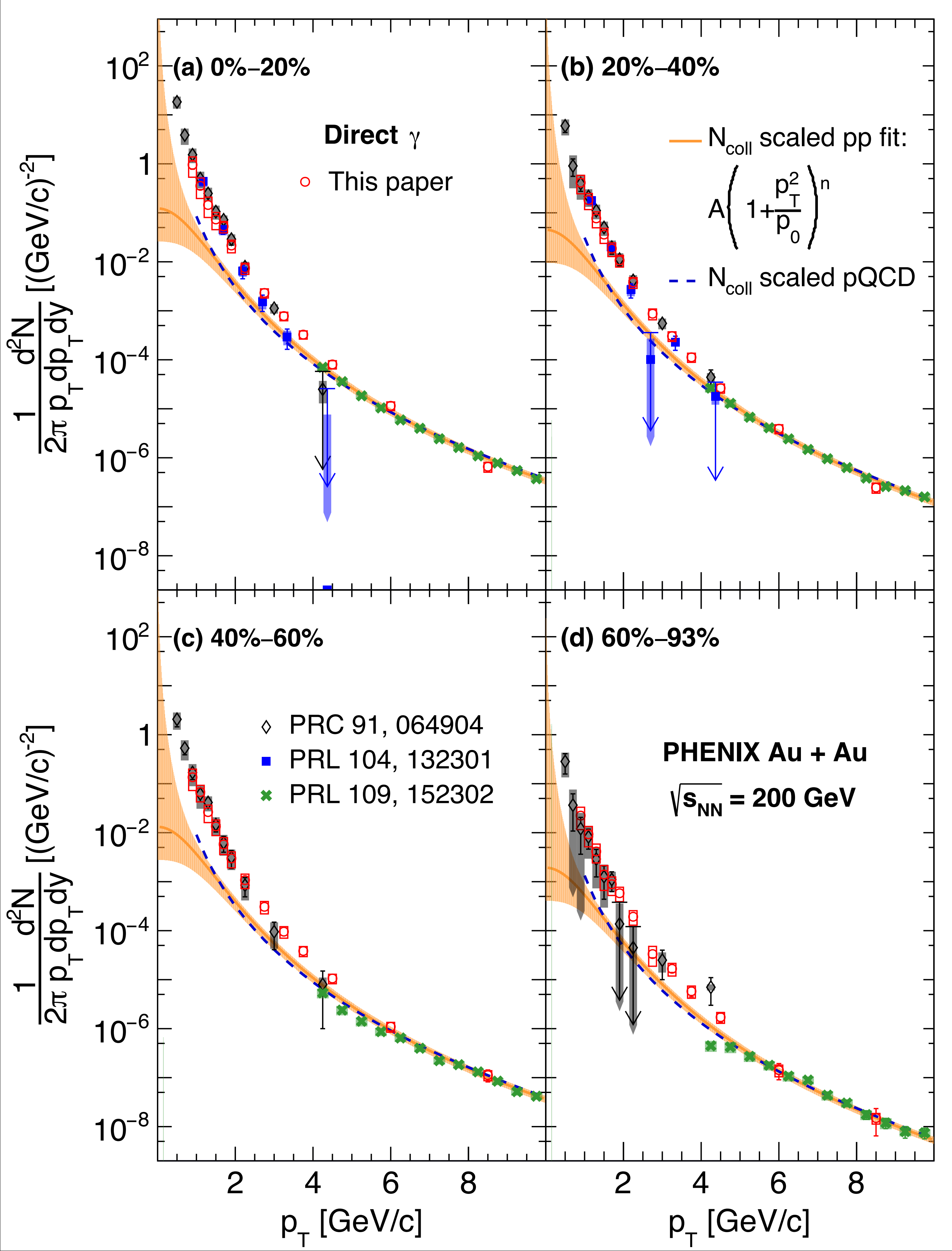

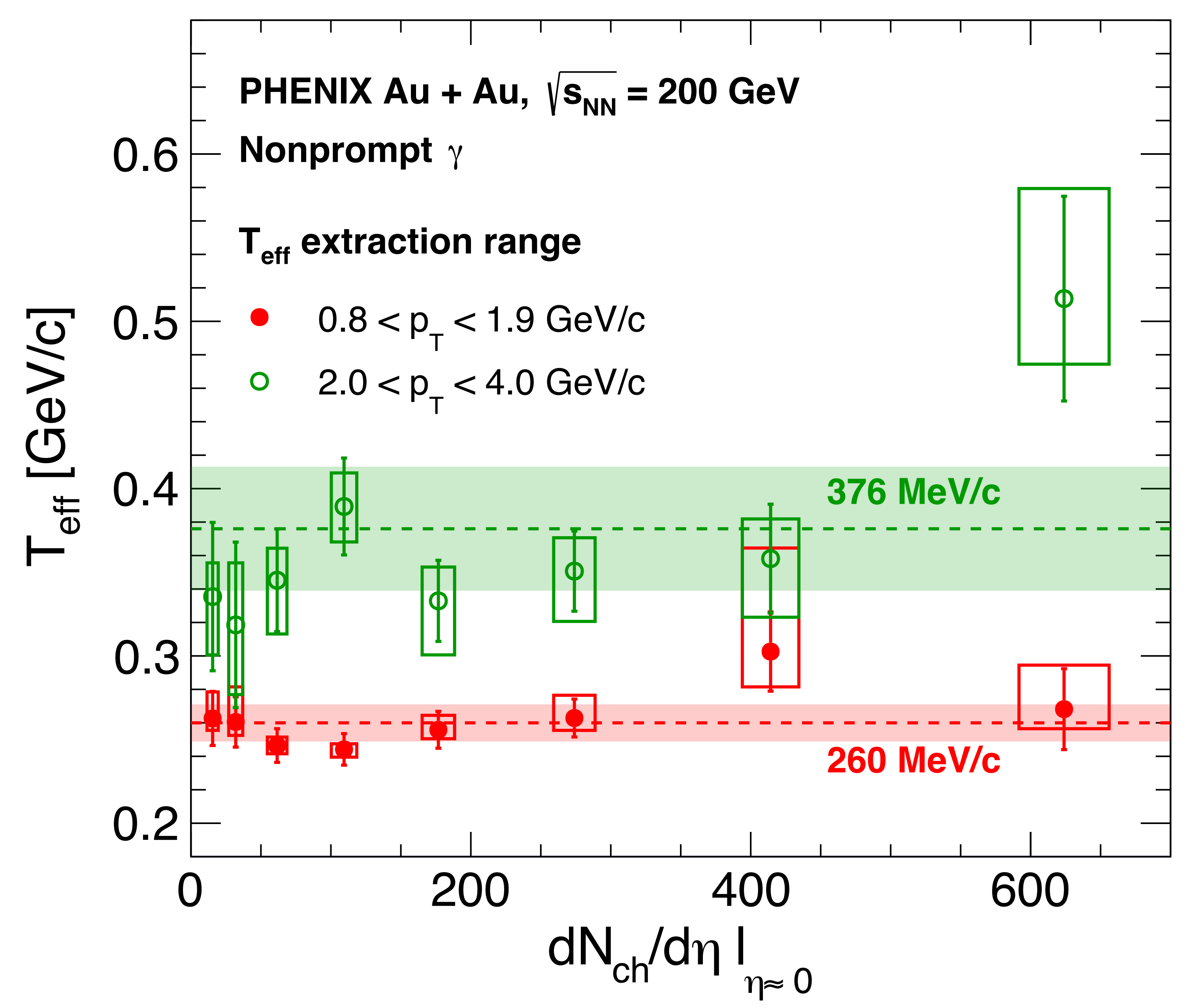

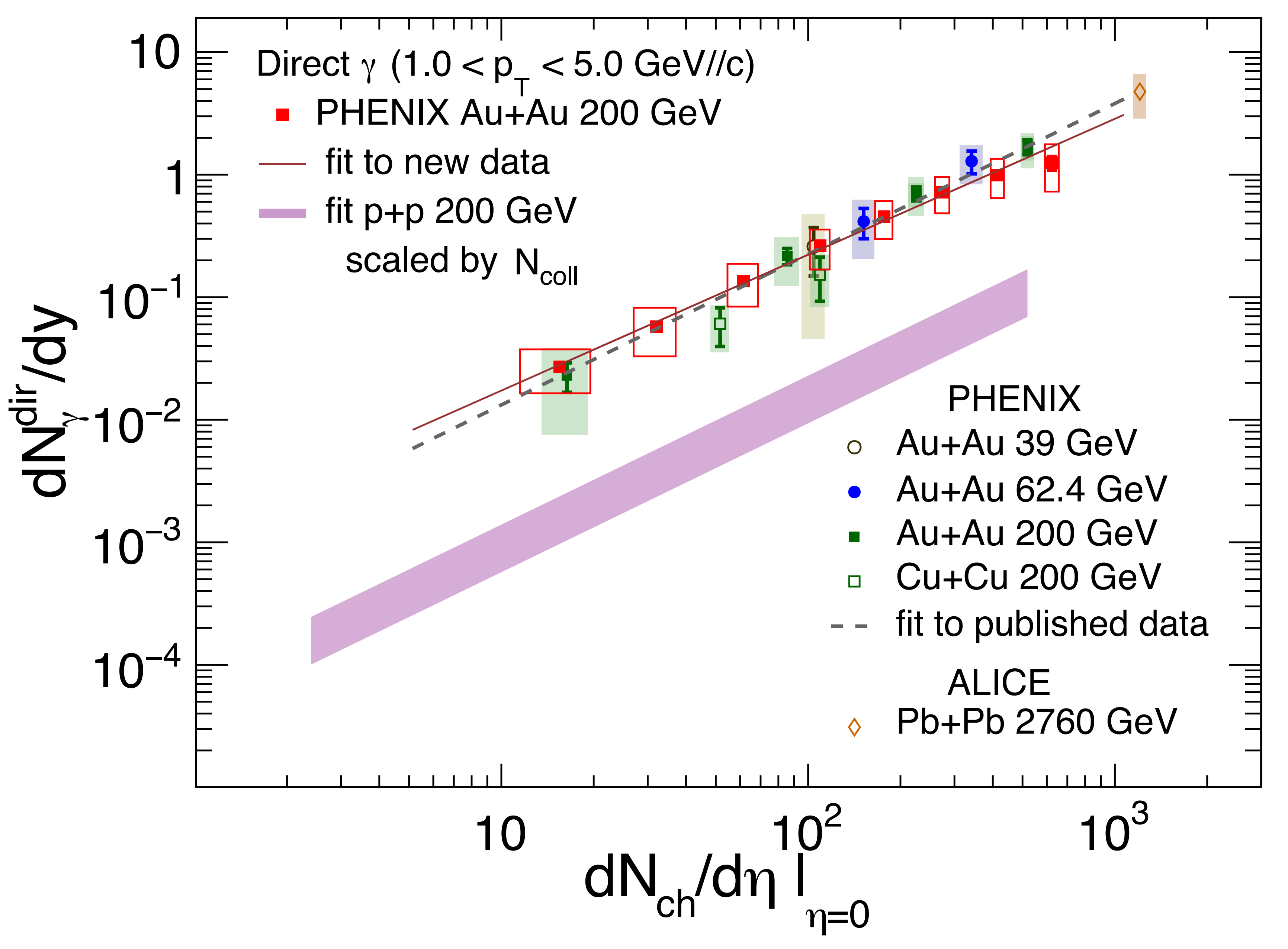

- Nonprompt direct γ obtained by subtracting the prompt component (N_{coll}-scaled direct γ from p+p collisions).
- Direct photon excess, above prompt-photon production from hard-scattering processes, observed for p_T < 6 GeV/c.

- Excess can be described by two exponentials with average inverse slopes T_{eff} = (260±11)MeV/c and T_{eff} = (376±37)MeV/c for (0.8< p_T <1.9) GeV/c and (2.0 < p_T <4.0) GeV/c, respectively.
- Integrated photon yield scales as $(dN_{ch}/d\eta)^{\alpha}$, α=1.12 ± 0.06(stat) ± 0.14(sys) with no apparent dependence on p_T.

2203.17187 [nucl-ex]

Medium temperature with di-leptons

Precision di-lepton spectra measured with Au+Au 27 GeV (2018) and 54.4 GeV data (2017)
blue-shift free average temperatures extracted: IMR systematically above LMR temperature

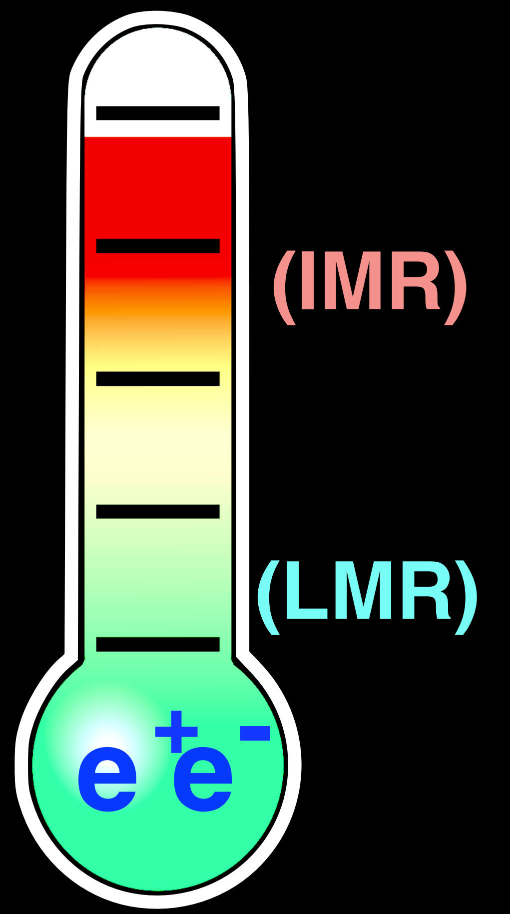

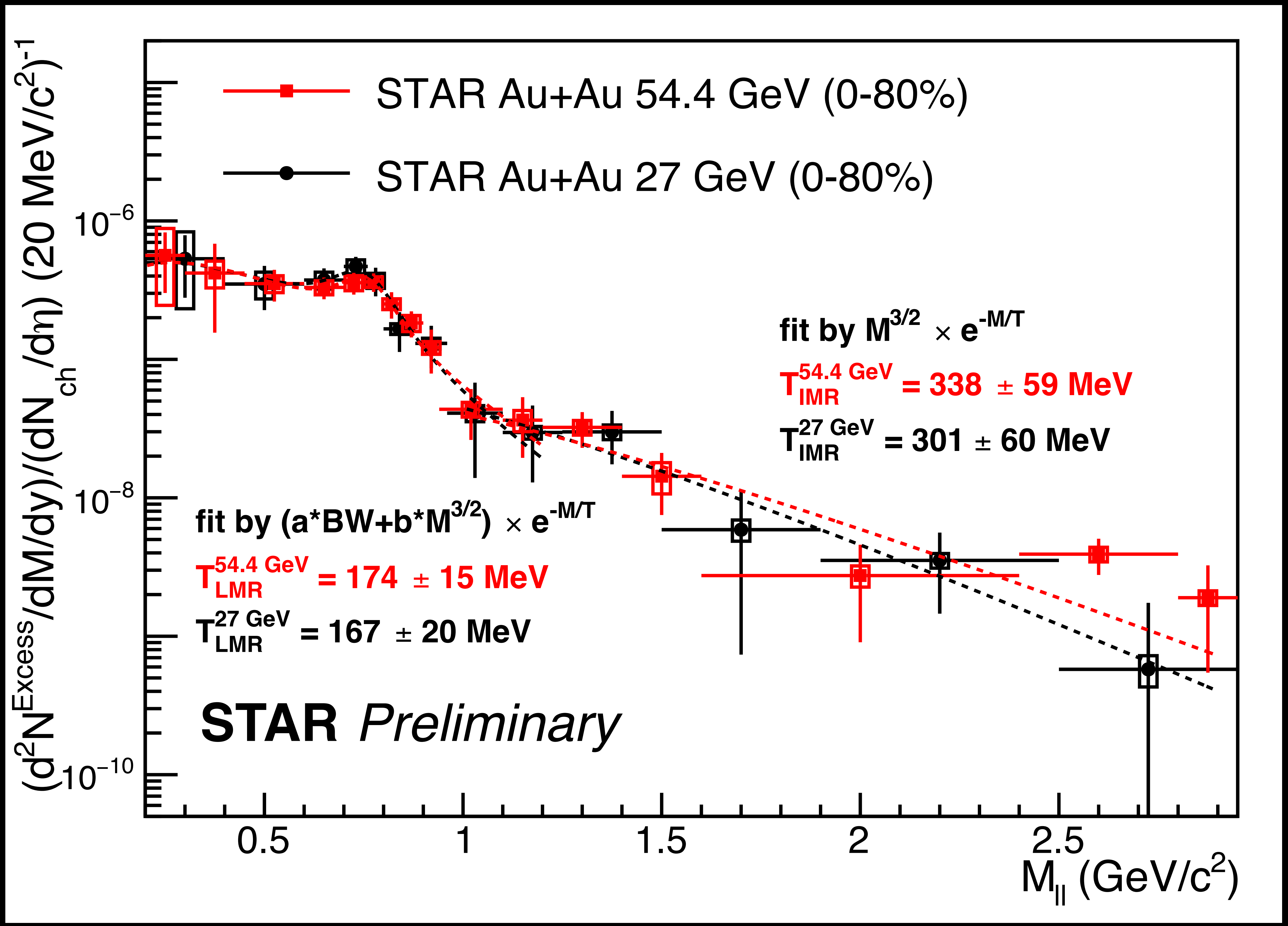

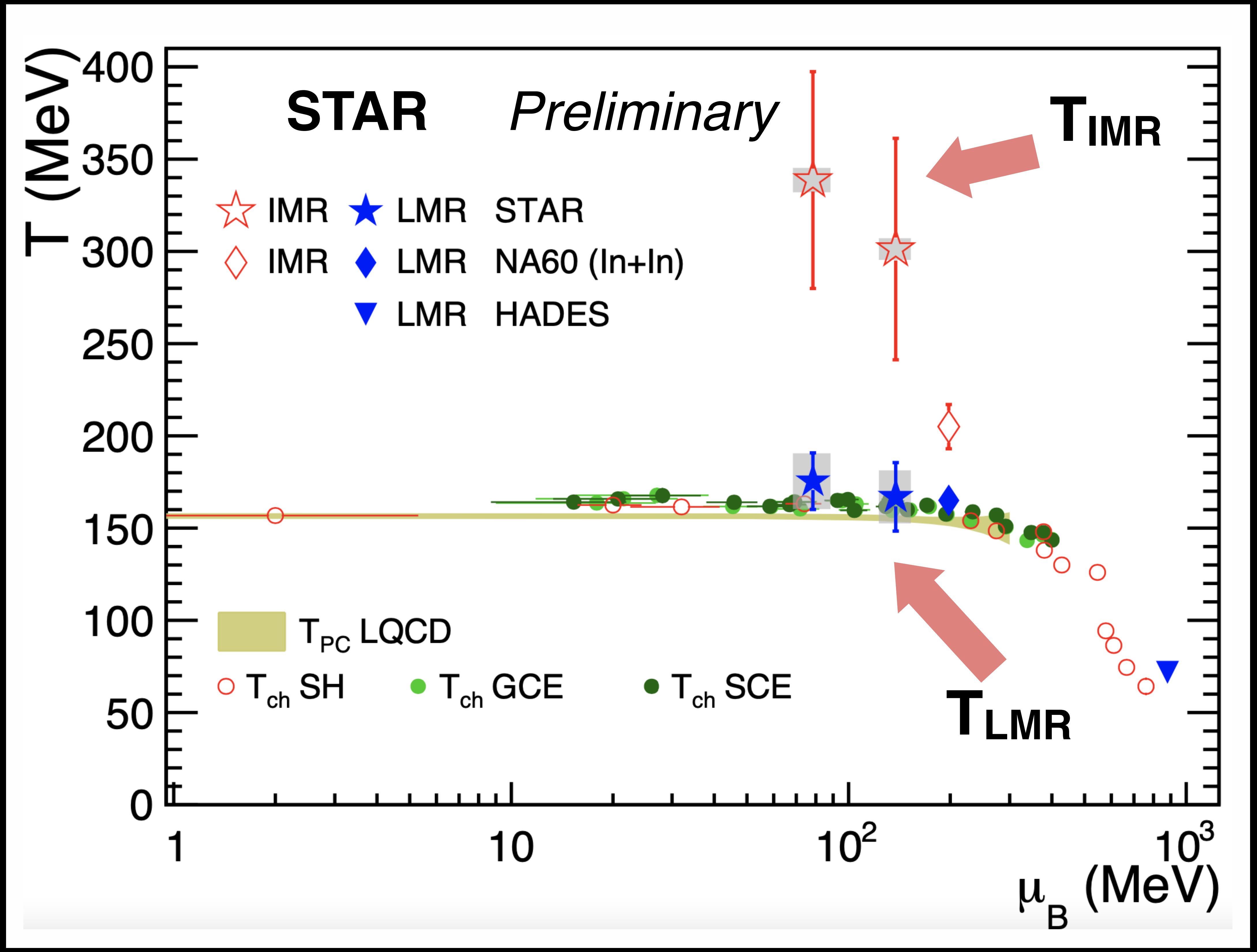

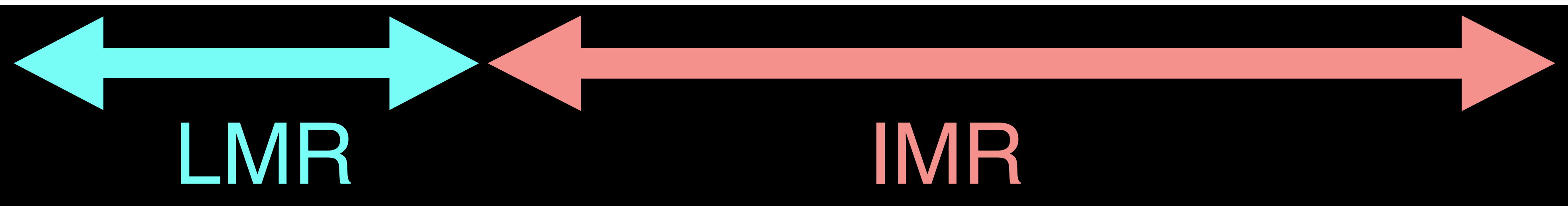

$T_{LMR} \sim T_{PC,LQCD}$ $T_{IMR} > T_{LMR}$

QGP temperature of ~300 MeV at 27 & 54.4 GeV extracted, ρ mediated di-leptons dominate near pseudo-critical temperature T_{PC} of the QCD chiral transition. Hot QCD Coll., Phys.Lett.B 795 (2019)15

Evidence for nonlinear gluon effects at small *x*

STAR: Phys.Rev.Lett. 129 (2022) 092501

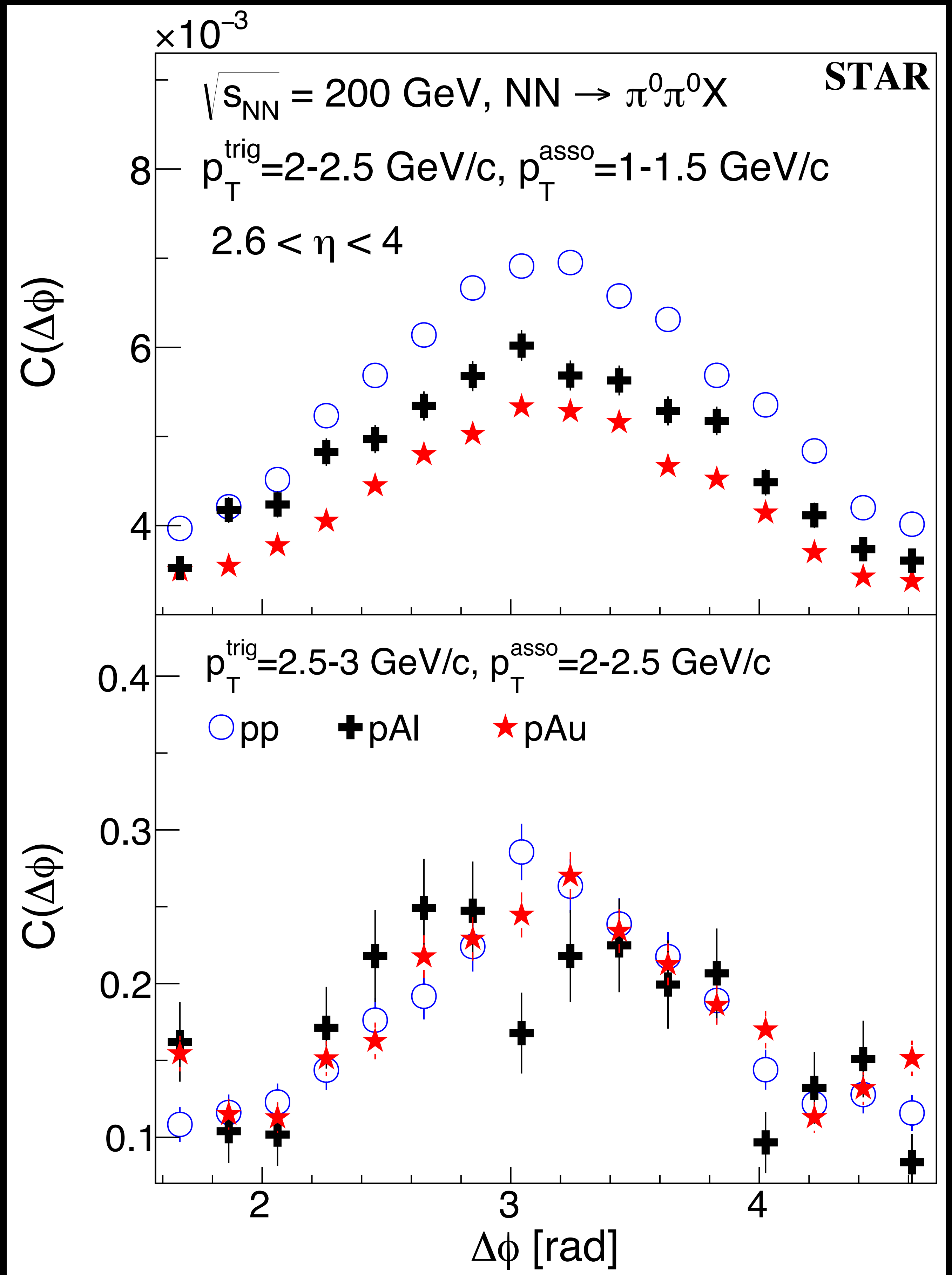

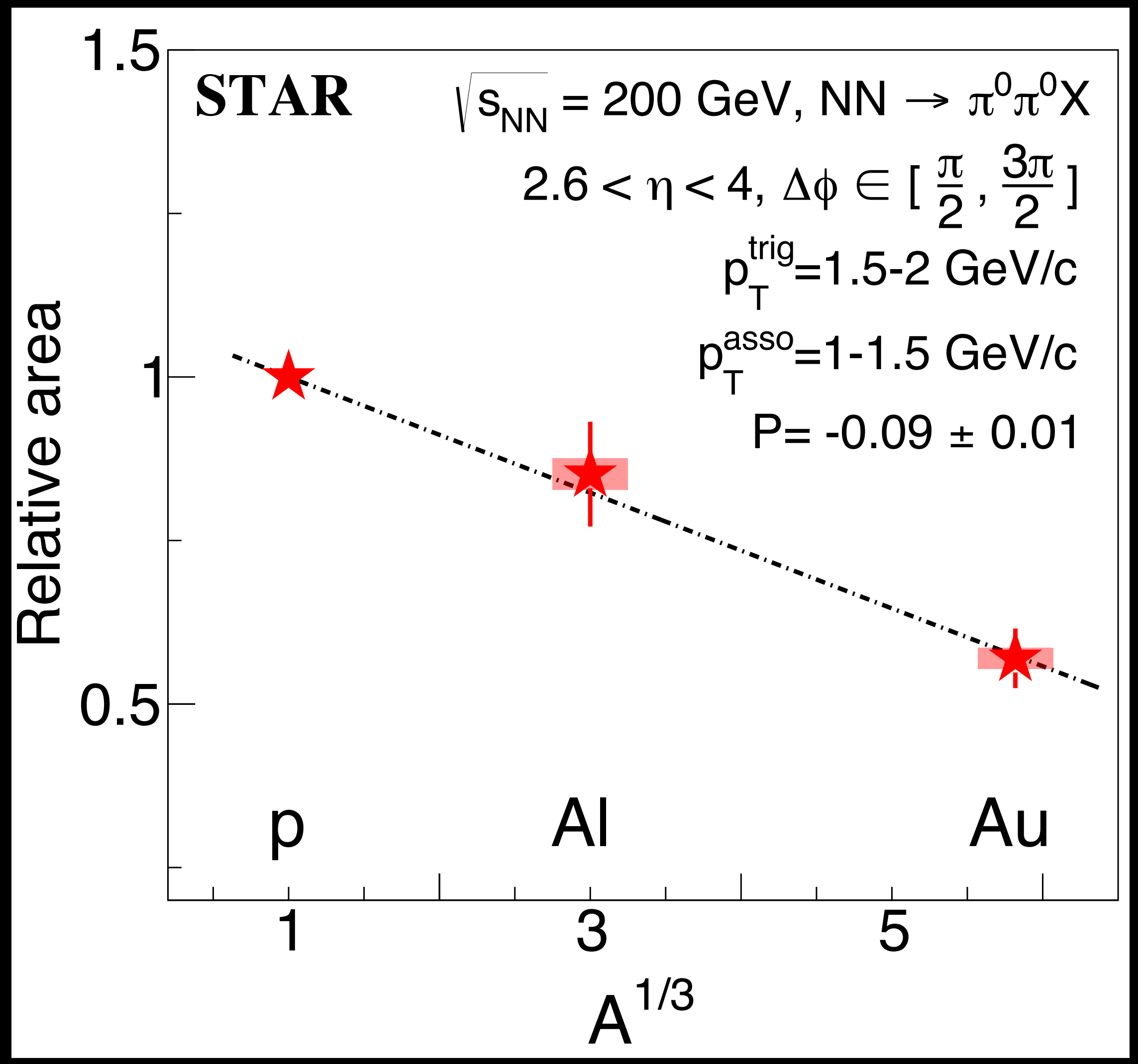

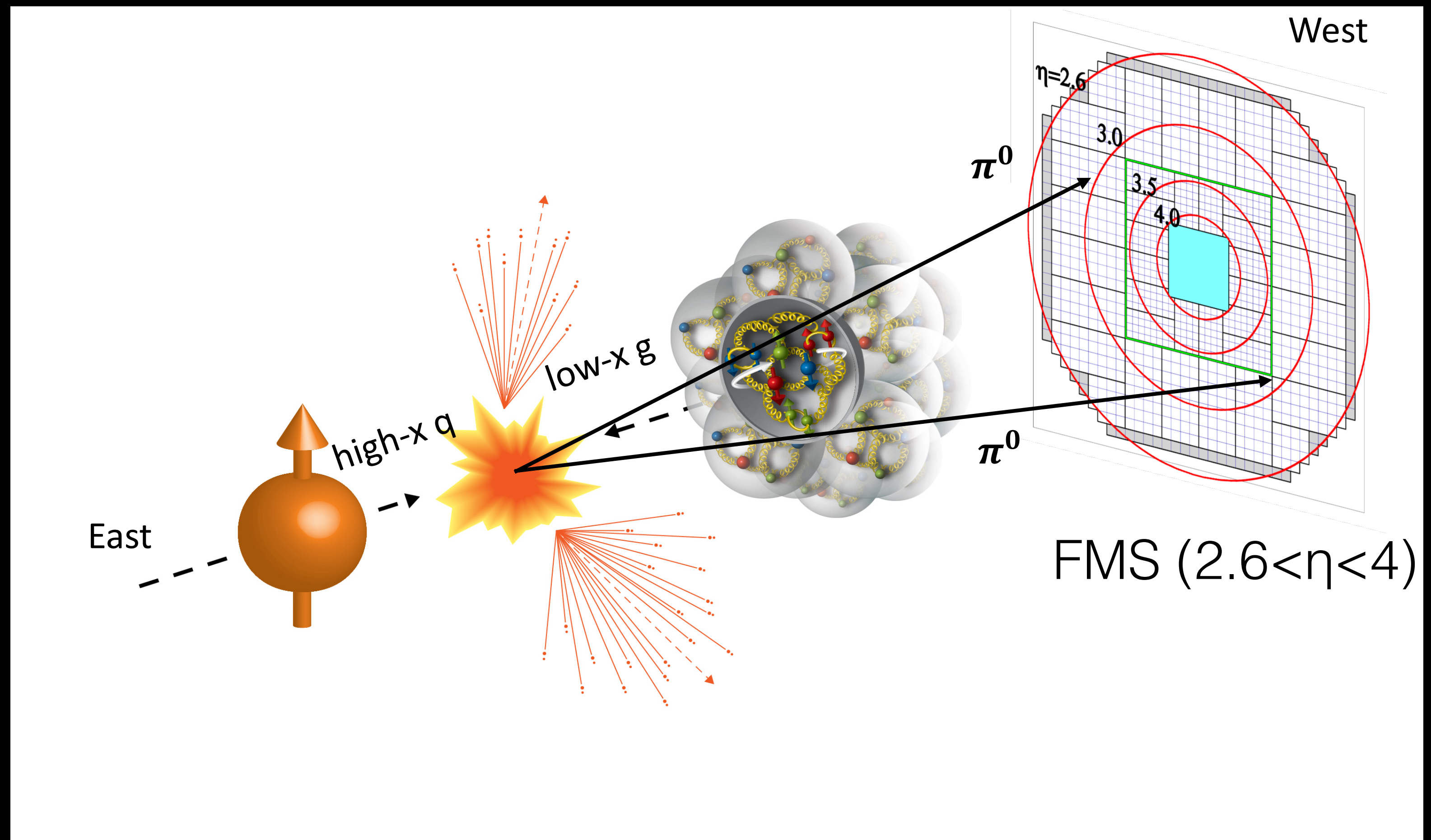

$$Q_s^2 \propto A^{1/3}(1/x)^{\lambda}$$

- π°-π° azimuthal correlations at forward rapidity (2.6 <η <4) probe high-density gluon field.
- Suppression of back-to-back pairs in pAl and pAu compared to pp with relative area ~ $A^{1/3}$, consistent with the expectation from gluon saturation.
  - No broadening of the away-side peak.
- Suppression decreases with increasing p_T.
- Future measurements: h-h and γ-h azimuthal correlations*.

I. Vitev, Phys. Lett. B 562, 36 (2003)

L. Frankfurt and M. Strikman, Phys. Lett. B 645, 412 (2007)

C. Marquet, Nuclear Physics A 796, 41 (2007), 0708.0231

L. Zheng, E. C. Aschenauer, J. H. Lee, and B.-W. Xiao, Phys. Rev. D 89, 074037 (2014), 1403.2413

) For γ(γ)-h azimuthal correlations a small dip at the maximum of C(Δφ) is expected (Stasto et al. 2012, Basso et al. 2016, Goncalves et al. 2020).

RHIC & EIC future schedule on the LHC timeline

RHIC in 2023-2025: sPHENIX & STAR

Unprecedented statistics to be collected for pp, pAu and AuAu collisions at 200 GeV

→ completion of RHIC mission

near-term mid-term

Forward upgrade program of STAR

SN0773 : The STAR BUR for Run-22 & data taking in 2023-25

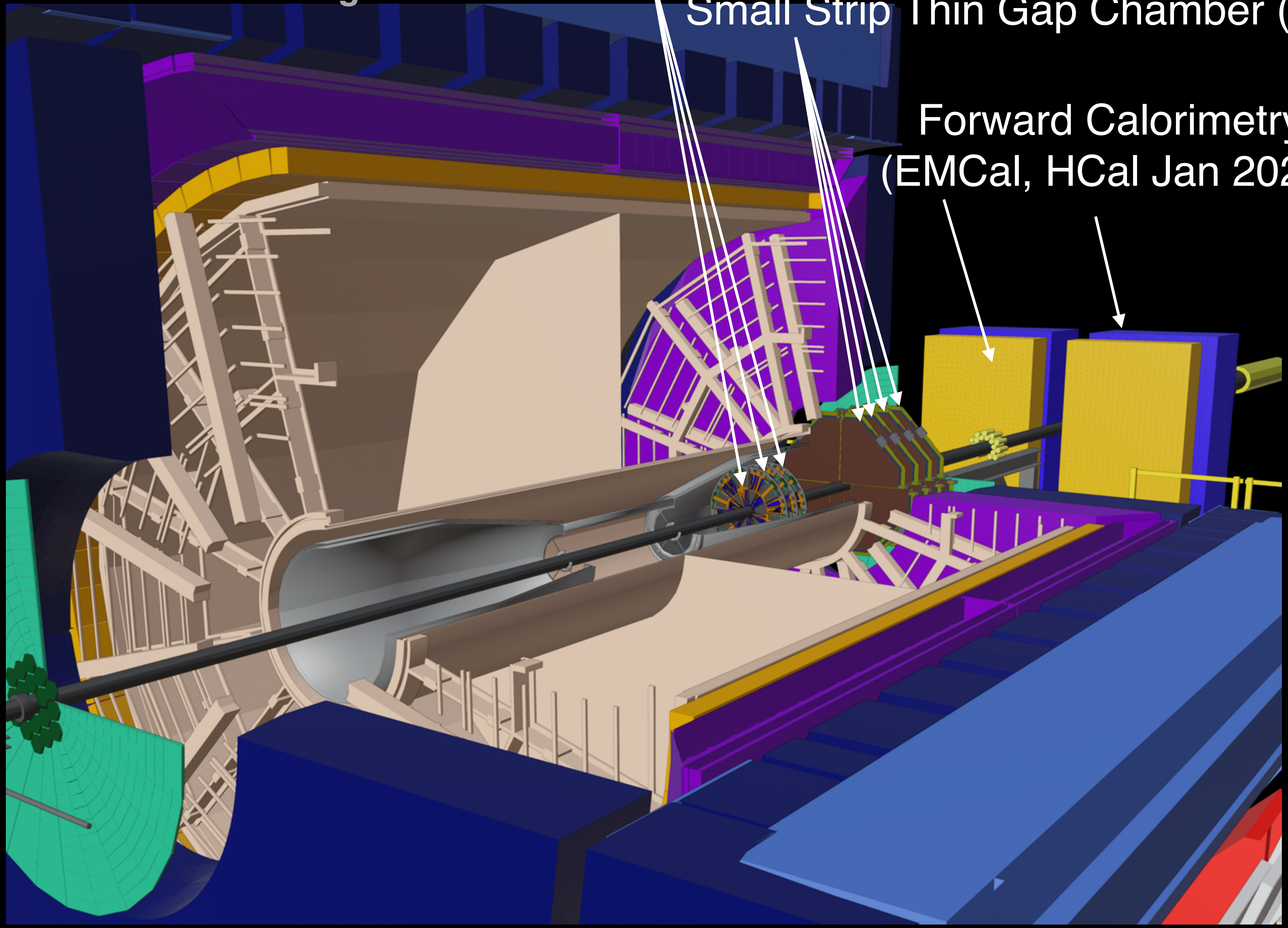

Anticipated runs with forward upgrades:
High statistics Au+Au in 2023 and 2025
Polarized p+p, p+Au in 2024

Di-hadron correlations studied in photonuclear processes using Au+Au $\sqrt{s_{NN}}$ = 54.4 GeV data

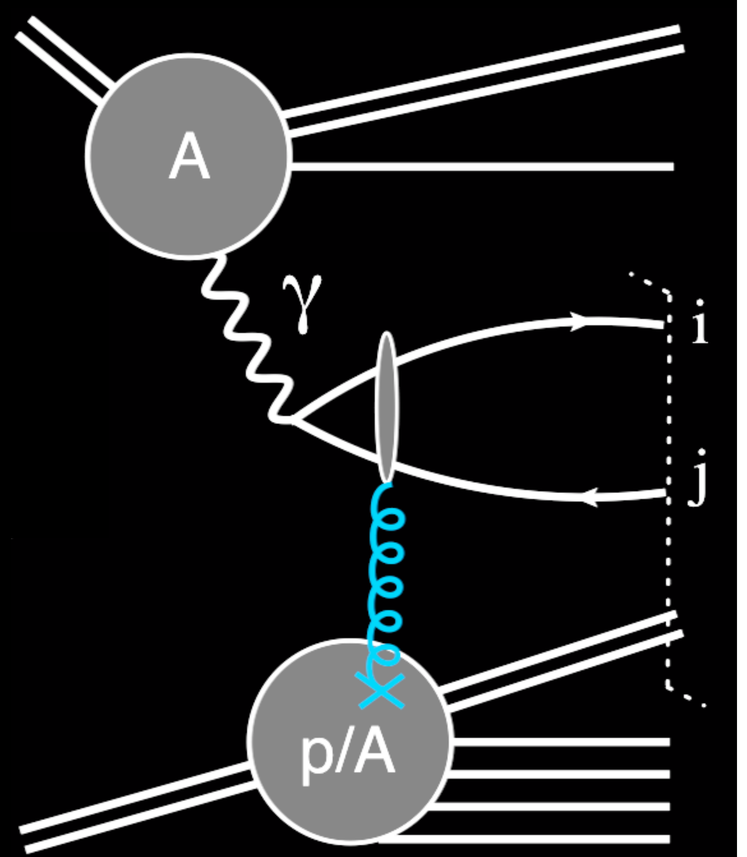

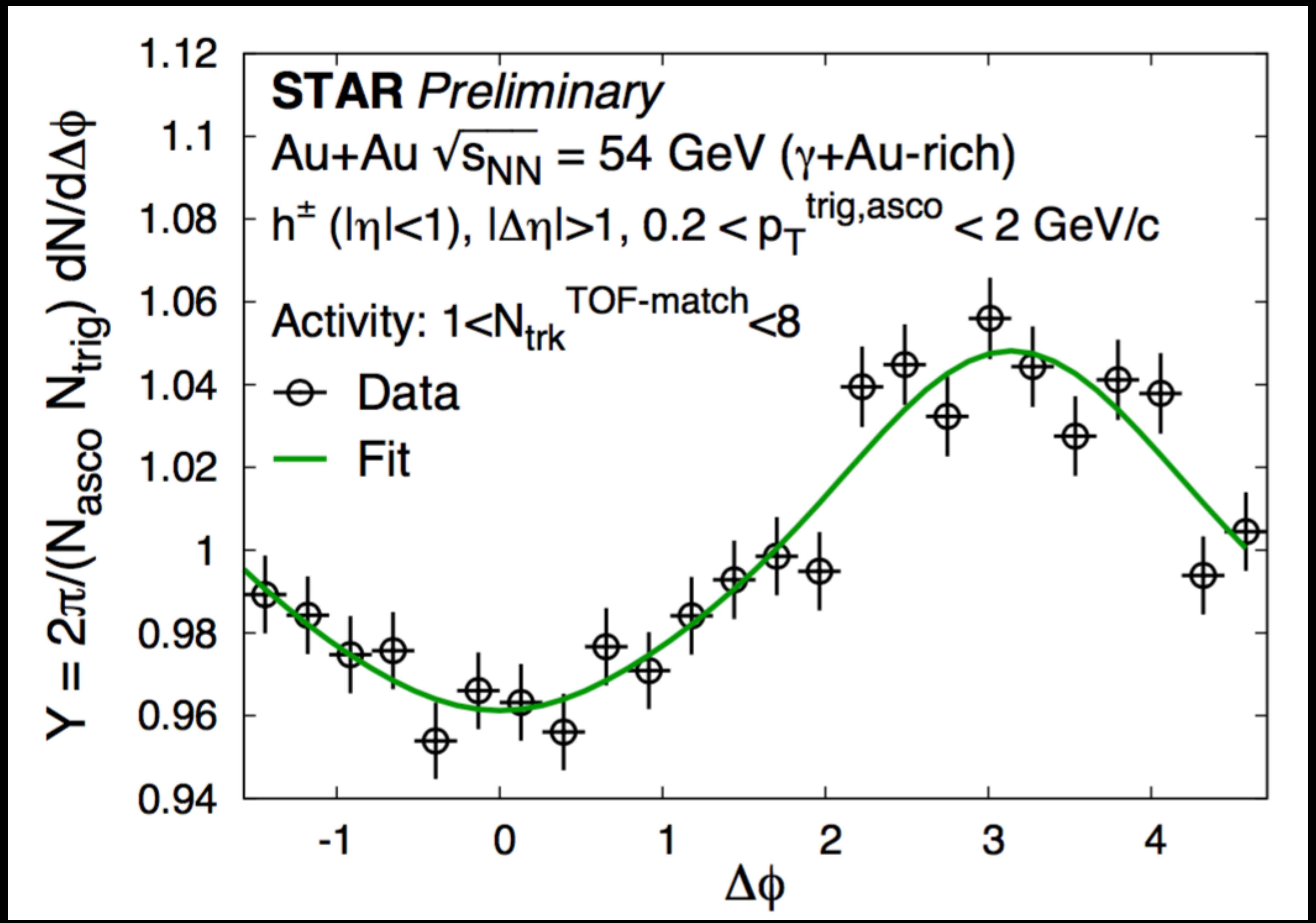

No signature of collectivity (near side ridge) in the γ+Au, higher energy and activity events under exploration with STAR forward upgrades

Focus will be on study of microstructure of QGP & RHIC measurements informative towards EIC science

sPHENIX - barrel detector with 4π coverage

($0<\phi<2\pi$, $|\eta|<0.85$)

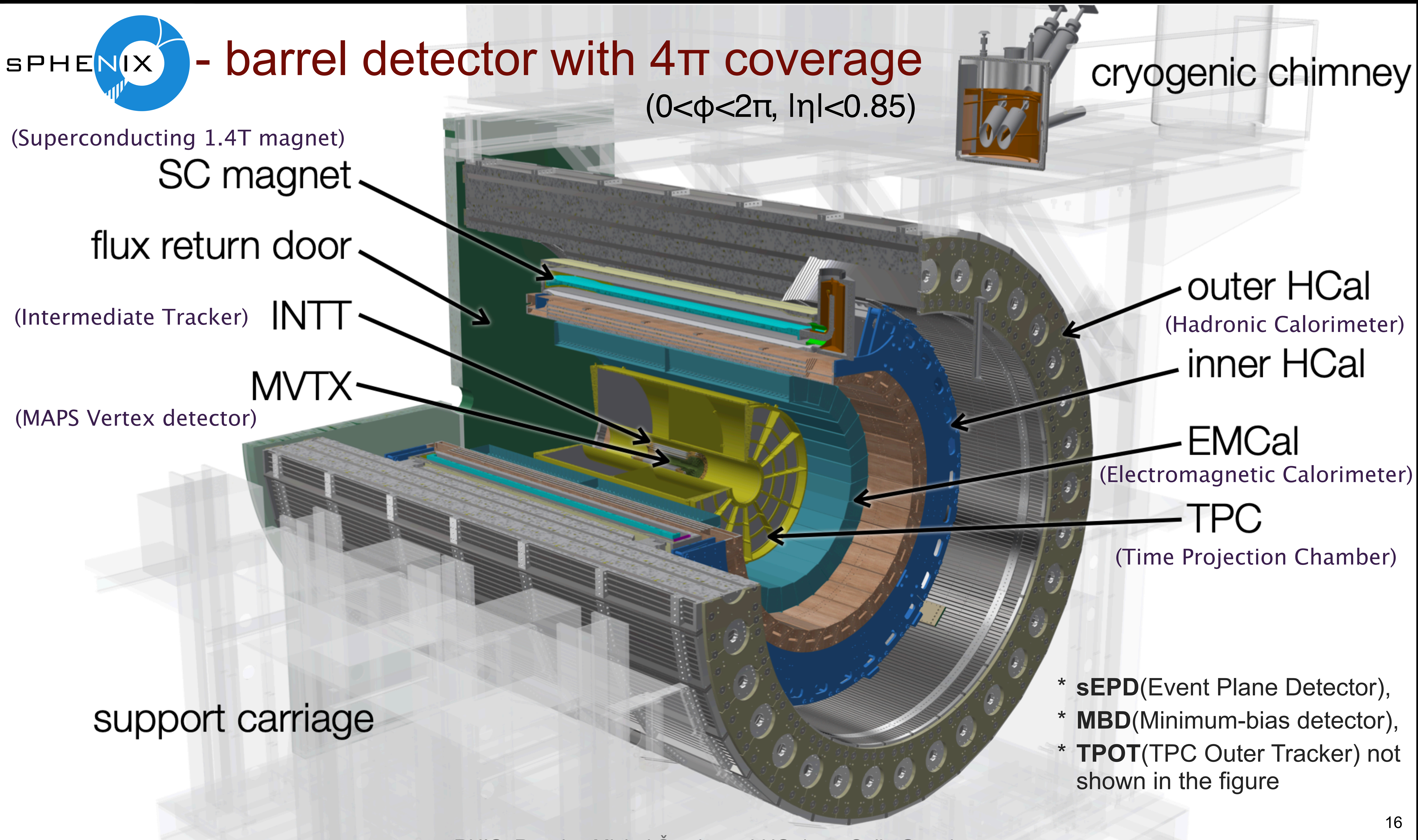

* **sEPD**(Event Plane Detector),
* **MBD**(Minimum-bias detector),
* **TPOT**(TPC Outer Tracker) not shown in the figure

Hard process yields

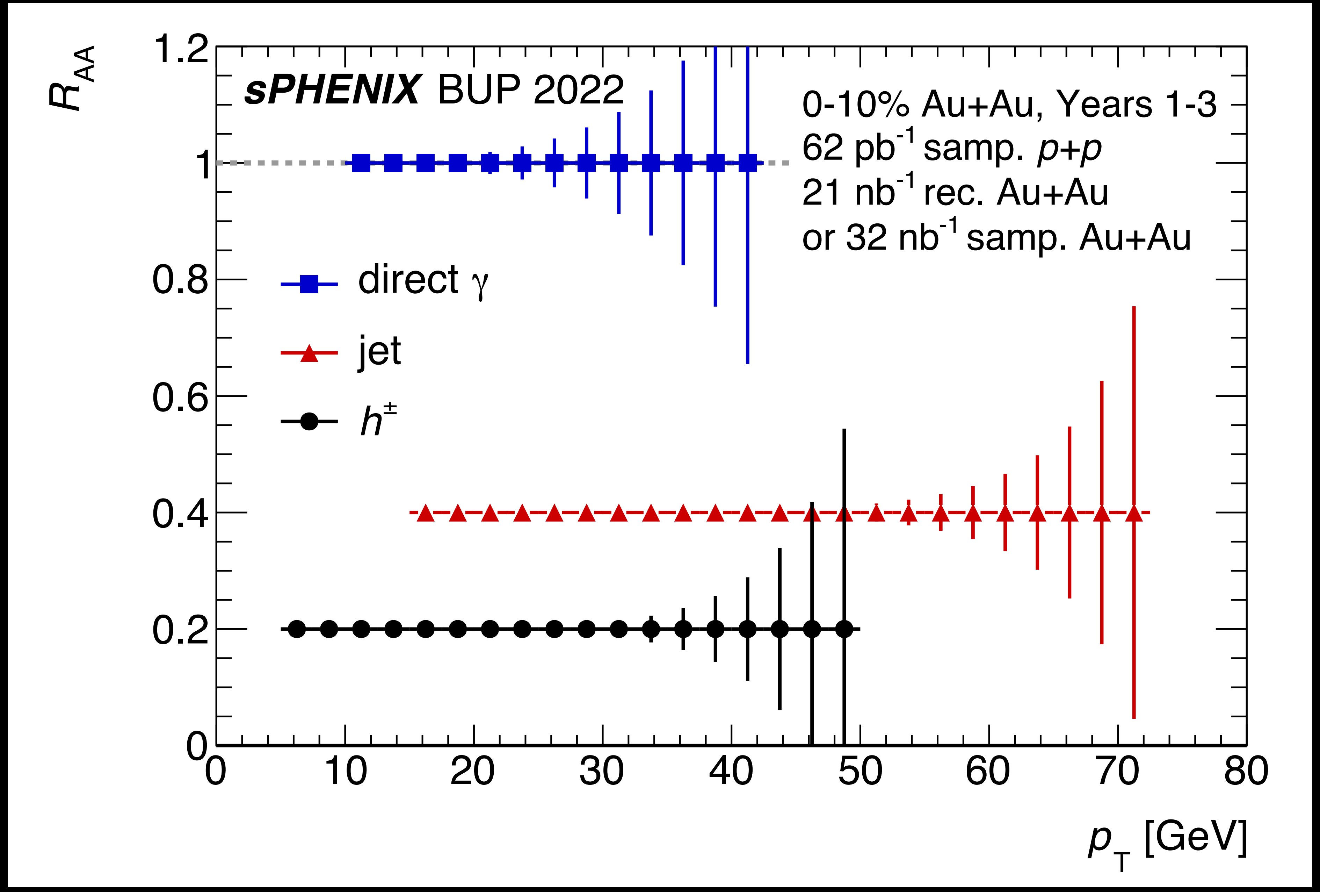

Signal	Au+Au 0–10% Counts	p+p Counts
Jets $p_T > 20$ GeV	22 000 000	11 000 000
Jets $p_T > 40$ GeV	65 000	31 000
Direct Photons $p_T > 20$ GeV	47 000	5 800
Direct Photons $p_T > 30$ GeV	2 400	290
Charged Hadrons $p_T > 25$ GeV	4 300	4 100

Table 4.1: Projected counts for jet, direct photon, and charged hadron events above the indicated threshold p_T from the sPHENIX proposed 2023–2025 data taking. These estimates correspond to the 28 cryo-week scenarios.

- Large luminosity for inclusive R_{AA} measurements (*left*) and detailed study (*right*)
  - ➡ **reconstructed jets** to ~70 GeV - fate of R_{AA} at very high p_T
  - ➡ **charged particles** to ~45 GeV - fragmentation functions out to high-z
  - ➡ **direct photons** to ~40 GeV - precise check of nuclear geometry

Thank you

Backup slides

Charged hadron R_{AA} at high p_T

Medium modification of J/ψ studied via R_{AA} in various systems at RHIC, new baseline measurement of R_{pA}

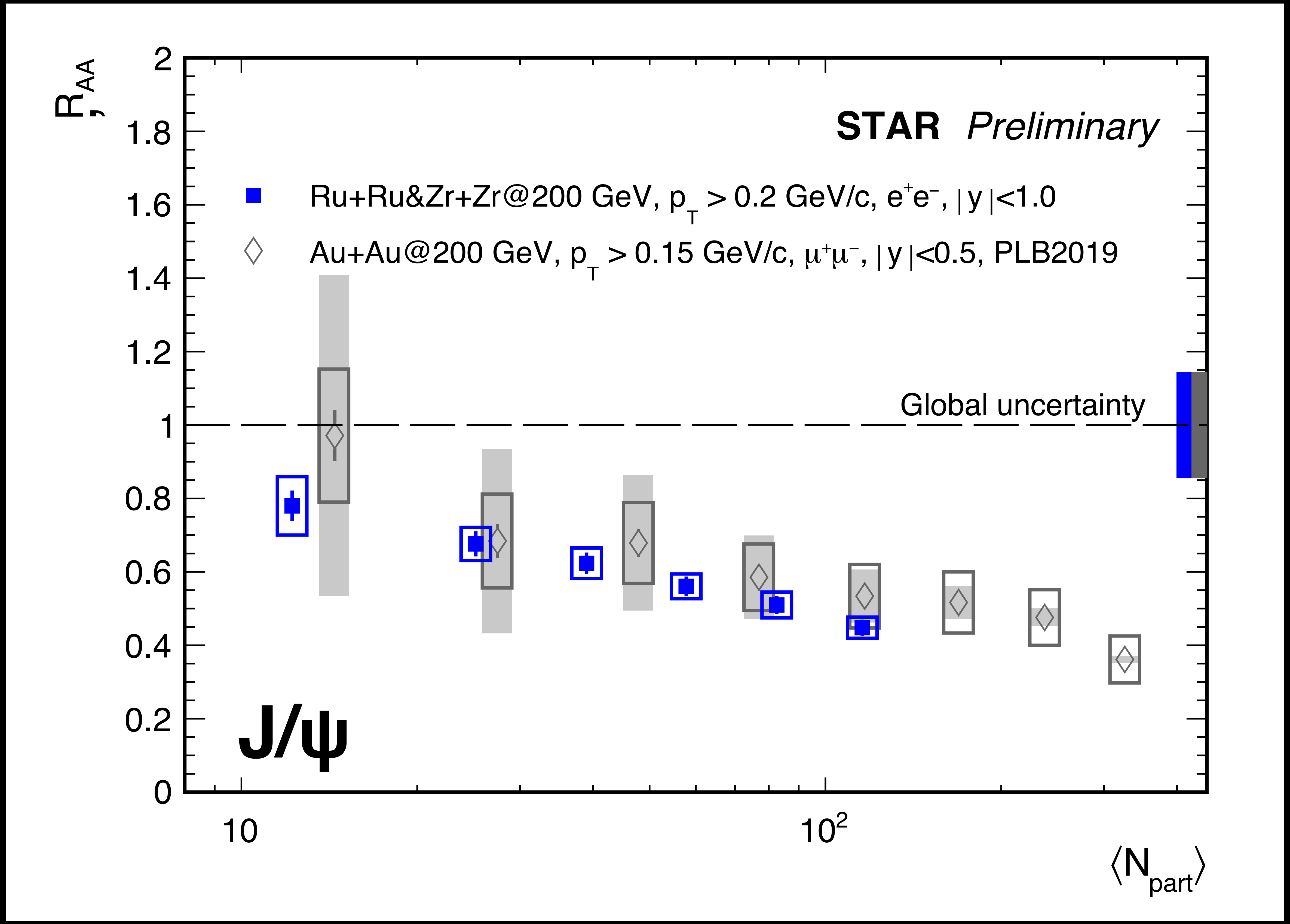

Medium modification of high p_T > 5 GeV/c hadrons studied via R_{AA} in isobars

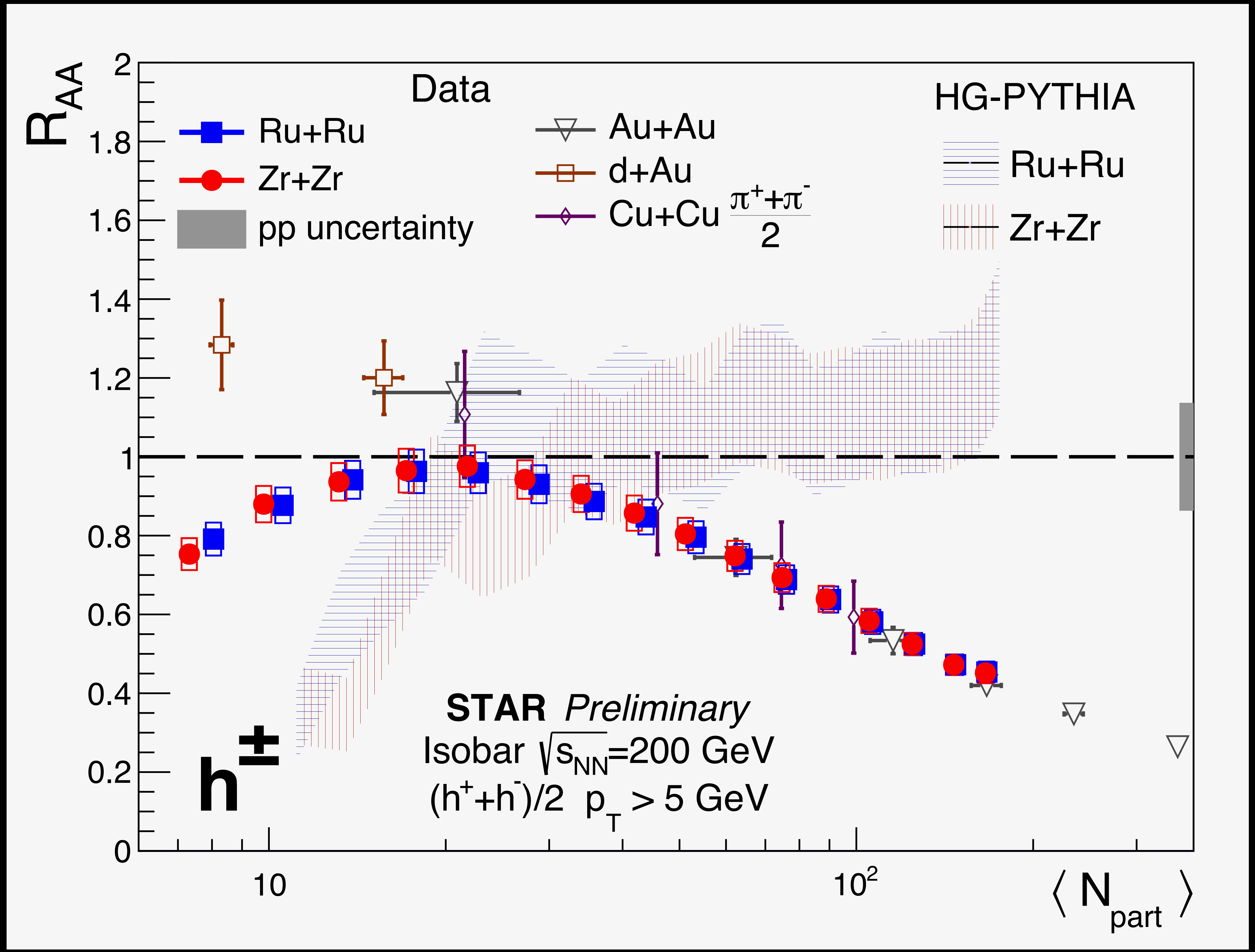

Clear indications of J/ψ suppression at RHIC that scales with N_{part}

Suppression of charged hadrons at high p_T possible centrality bias in peripheral events

Open heavy flavor tagged jets

First measurement of D^0-tagged jets@RHIC using STAR HFT

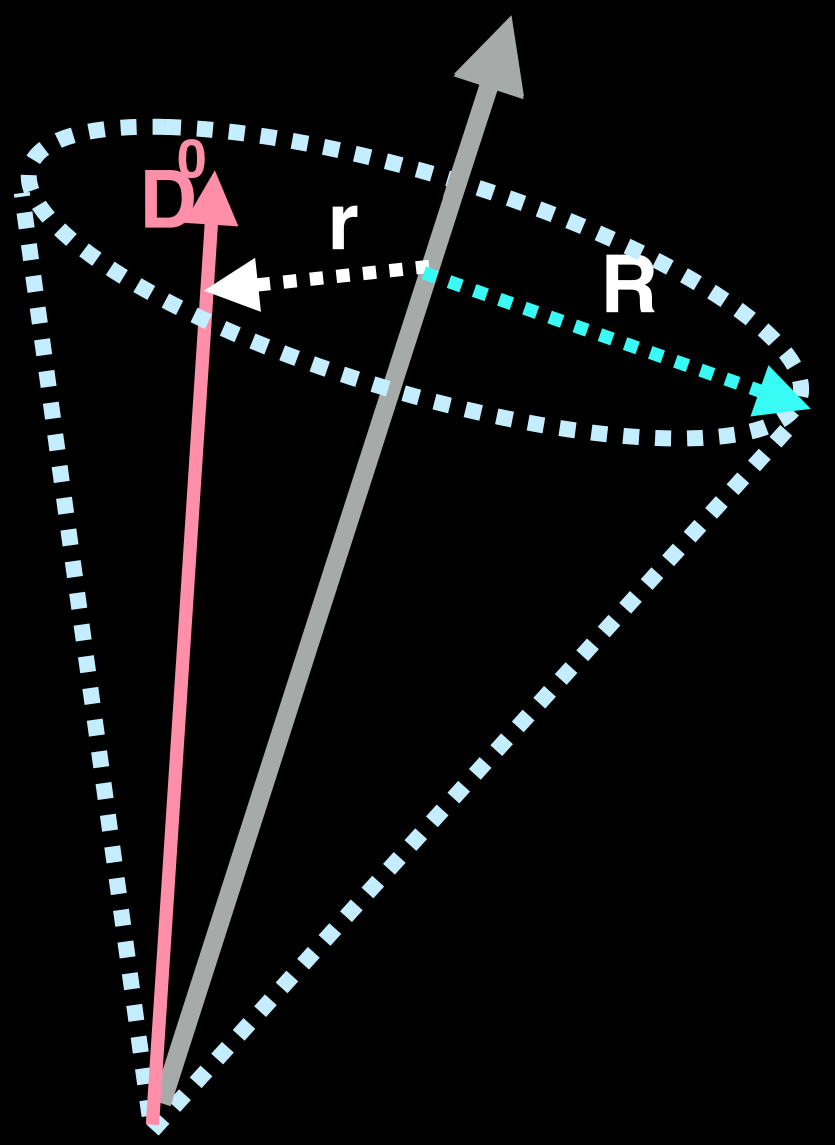

PYTHIA fragmentation is used for unfolding

R^*_{CP} in mid-central & central events indicate suppression at low jet-p_T

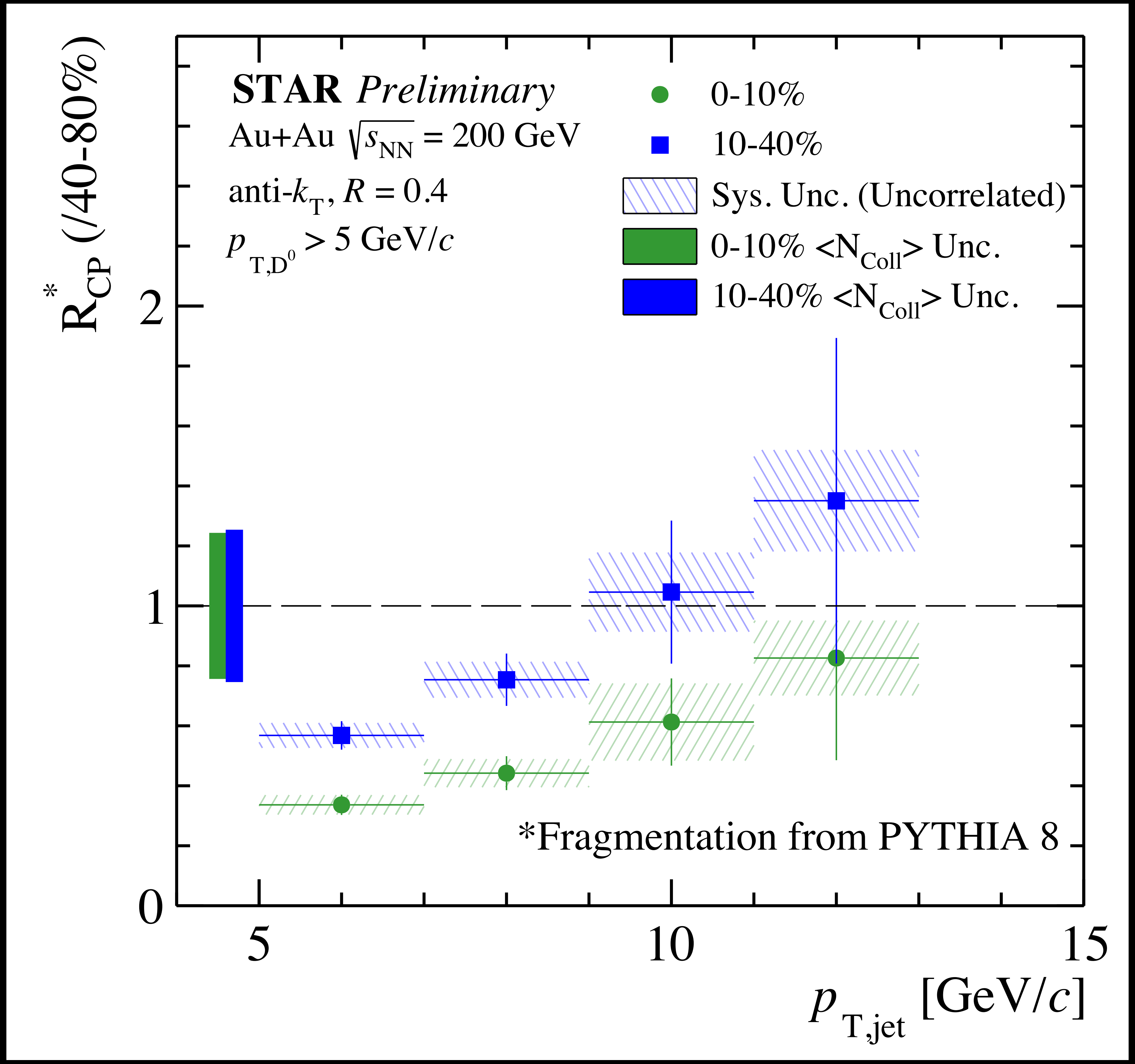

No jet substructure modification seen in central & mid-central events within uncertainties

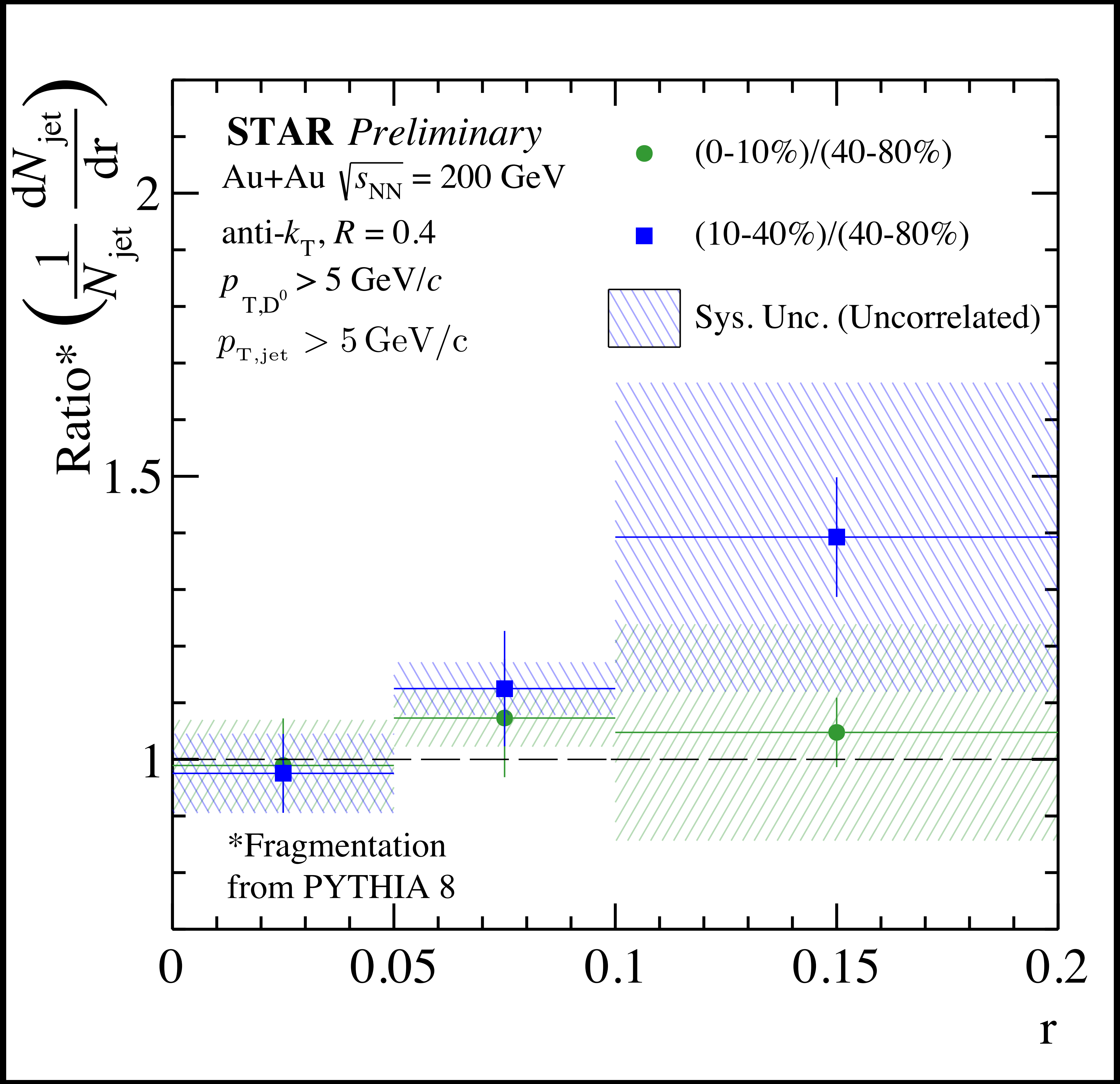

Access to mechanisms of heavy quark diffusion & ene

Chiral magnetic effect search in isobar collisions

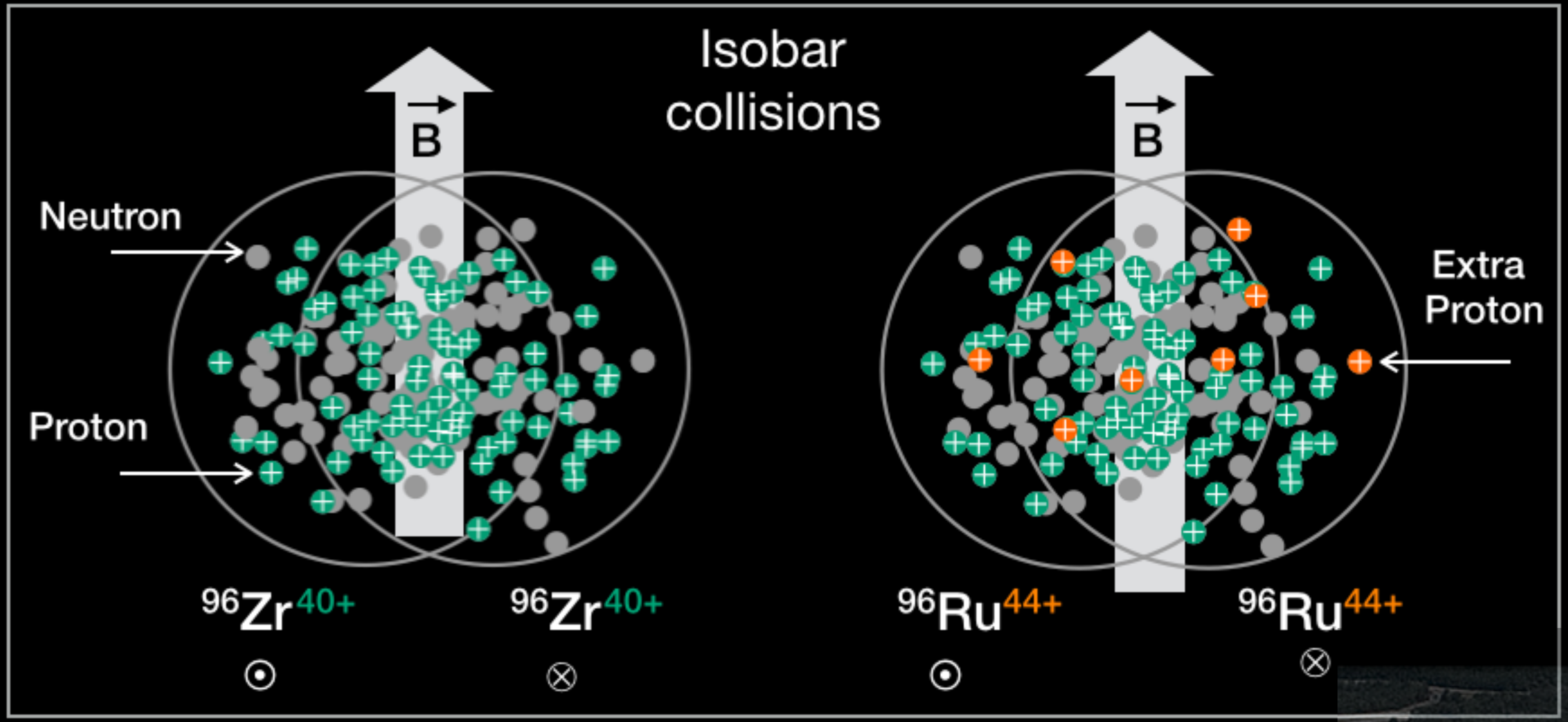

Biot-Savarat: $B_\perp = \gamma Z e \frac{b}{R^3} = \frac{\sqrt{s_{NN}}}{2m_N} Z e \frac{b}{R^3}$

Au+Au: $\gamma = 100,\ Z = 79,\ b = R_A = 7fm \Rightarrow eB = 10^{18}G$

B-field square is 10-15% larger in Ru+Ru than Zr+Zr

$$\frac{\langle \mathrm{Observable} \rangle_{\mathrm{Ru+Ru}}}{\langle \mathrm{Observable} \rangle_{\mathrm{Zr+Zr}}} > 1$$

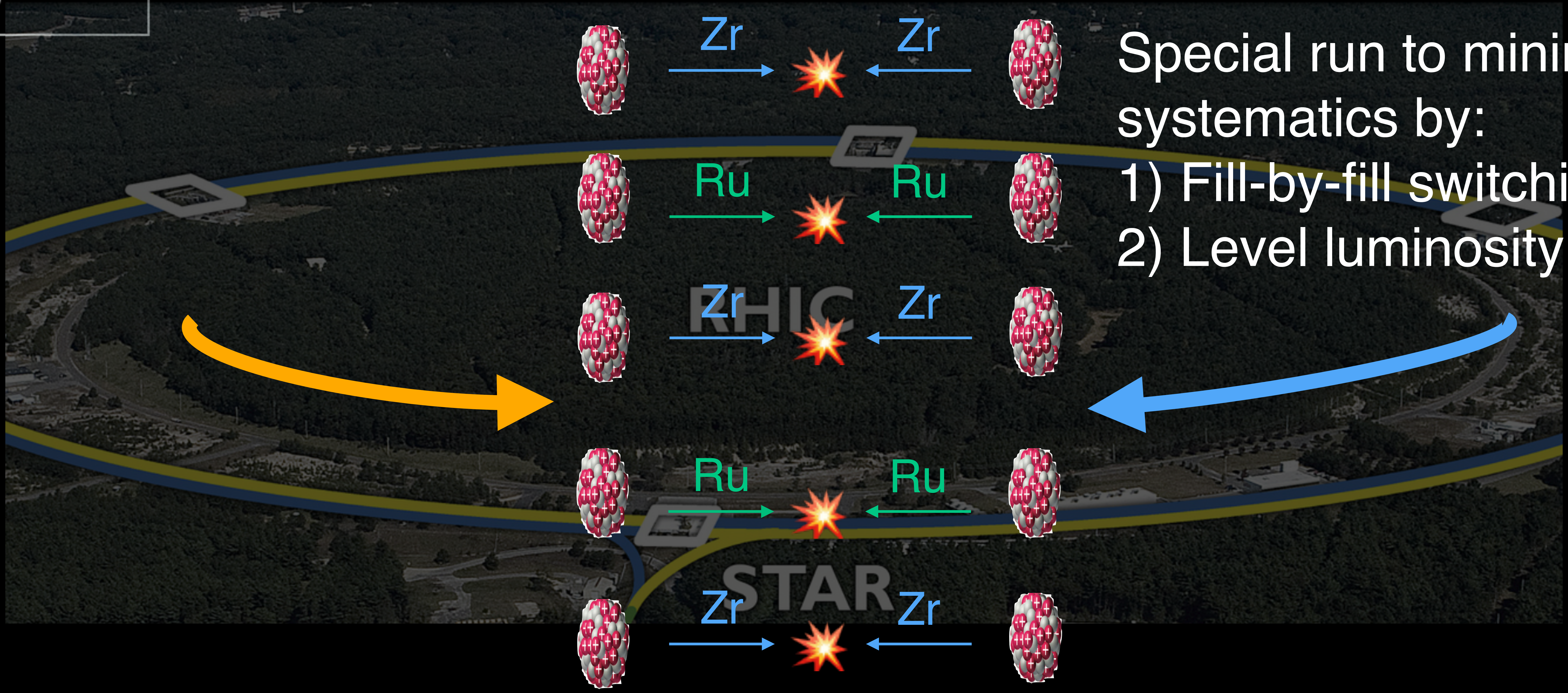

Special run to minimize systematics by:

1) Fill-by-fill switching
2) Level luminosity

Best possible control of signal and background compared to all previous experiments for CME search

e-Print: 2208.09069 [nucl-ex]

Chiral magnetic effect search in isobar collisions

STAR

Blind analysis performed with pre-defined criteria for primary CME sensitive observable:

$$\frac{(\Delta\gamma/v_2)_{\mathrm{Ru+Ru}}}{(\Delta\gamma/v_2)_{\mathrm{Zr+Zr}}} \approx 1 + f_{\mathrm{CME}}^{\mathrm{Zr+Zr}}[\underbrace{(B_{\mathrm{Ru+Ru}}/B_{\mathrm{Zr+Zr}})^2 - 1}_{0.1\text{-}0.15}] > 1 \text{ (for CME)}$$

$f_{\mathrm{CME}}^{\mathrm{Zr+Zr}}$: Unknown

Precision of 0.4% achieved

M. Abdallah et al. (STAR Collaboration), Phys. Rev. C 105 (2022) 1, 014901

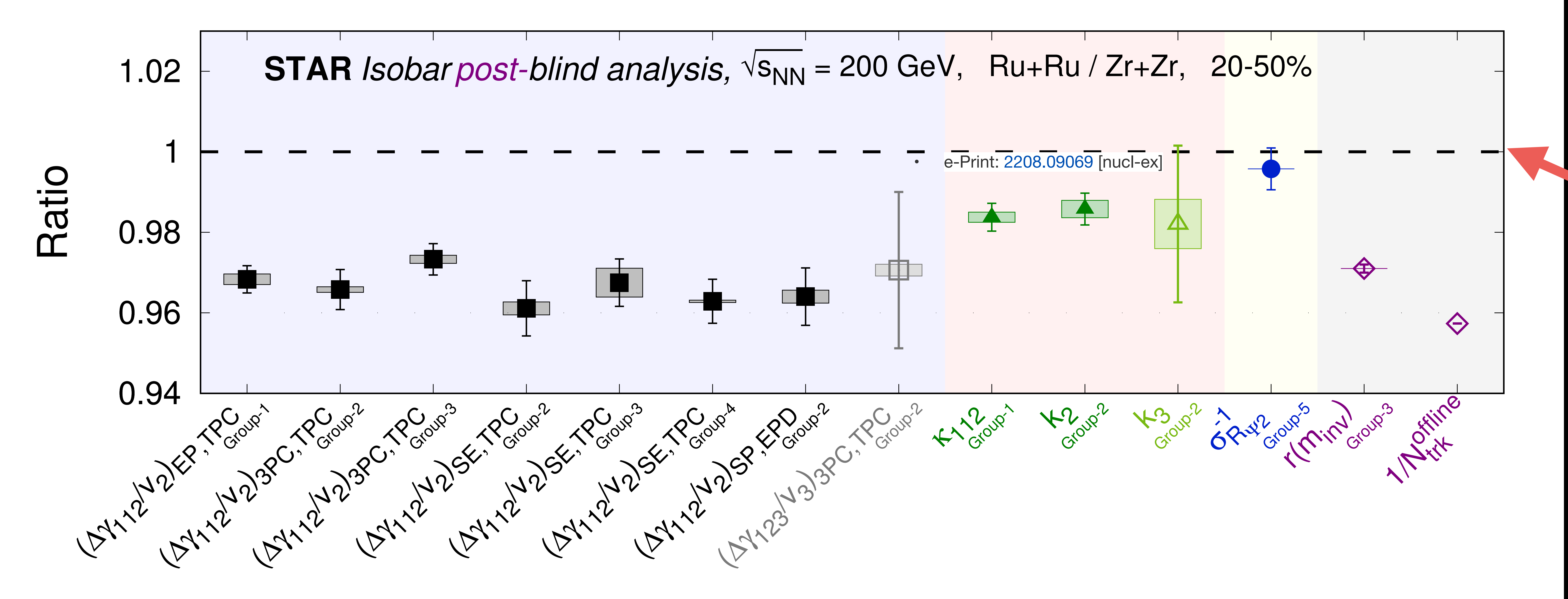

Blind analysis baseline

No pre-defined signature of CME is observed in isobar collisions, possible residual signal due to change of baseline & non-flow effects are under study

e-Print: 2208.09069 [nucl-ex]

Chiral magnetic effect search in isobar collisions

STAR

Blind analysis performed with pre-defined criteria for primary CME sensitive observable:

$$\frac{(\Delta\gamma/v_2)_{\mathrm{Ru+Ru}}}{(\Delta\gamma/v_2)_{\mathrm{Zr+Zr}}} \approx 1 + f_{\mathrm{CME}}^{\mathrm{Zr+Zr}}[\underbrace{(B_{\mathrm{Ru+Ru}}/B_{\mathrm{Zr+Zr}})^2 - 1}_{0.1\text{-}0.15}] > 1 \ (\text{for CME})$$

$f_{\mathrm{CME}}^{\mathrm{Zr+Zr}}$ ↑ Unknown

Precision of 0.4% achieved

M. Abdallah et al. (STAR Collaboration), Phys. Rev. C 105 (2022) 1, 014901

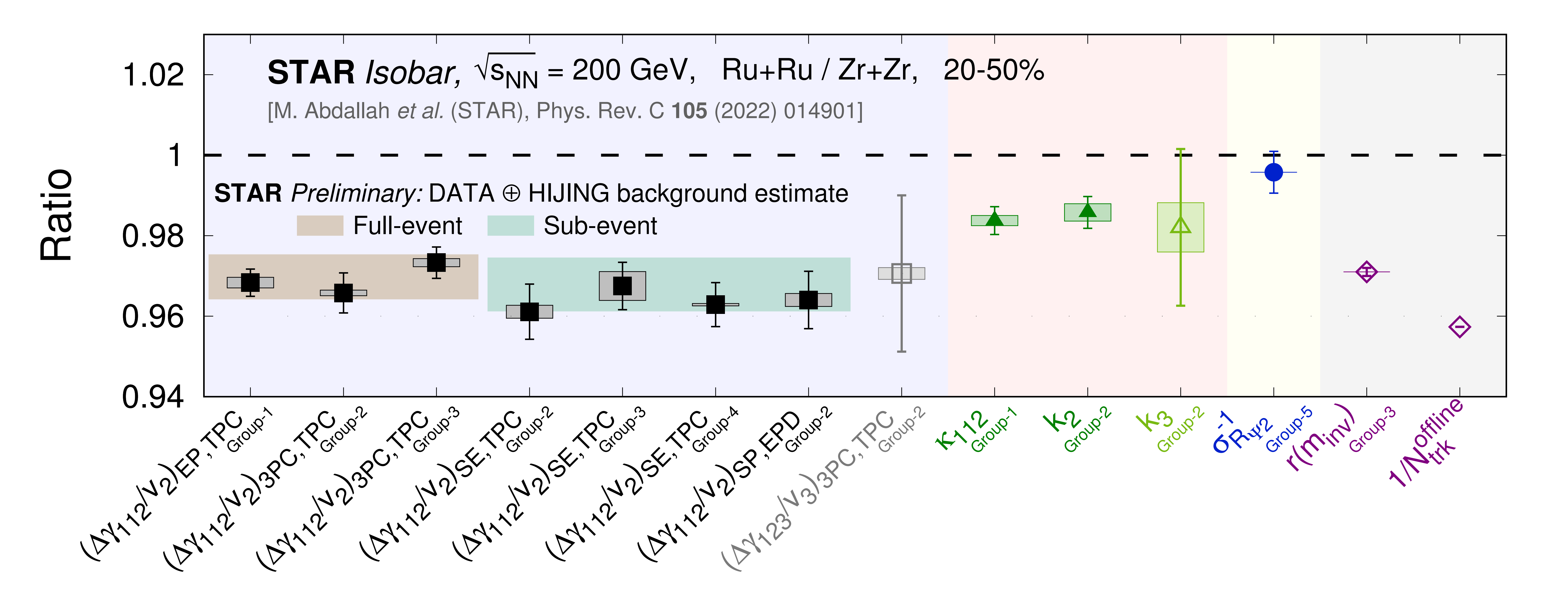

No pre-defined signature of CME is observed in isobar collisions, possible residual signal due to change of baseline & non-flow effects are under study

e-Print: 2208.09069 [nucl-ex]

Global spin alignment of vector mesons

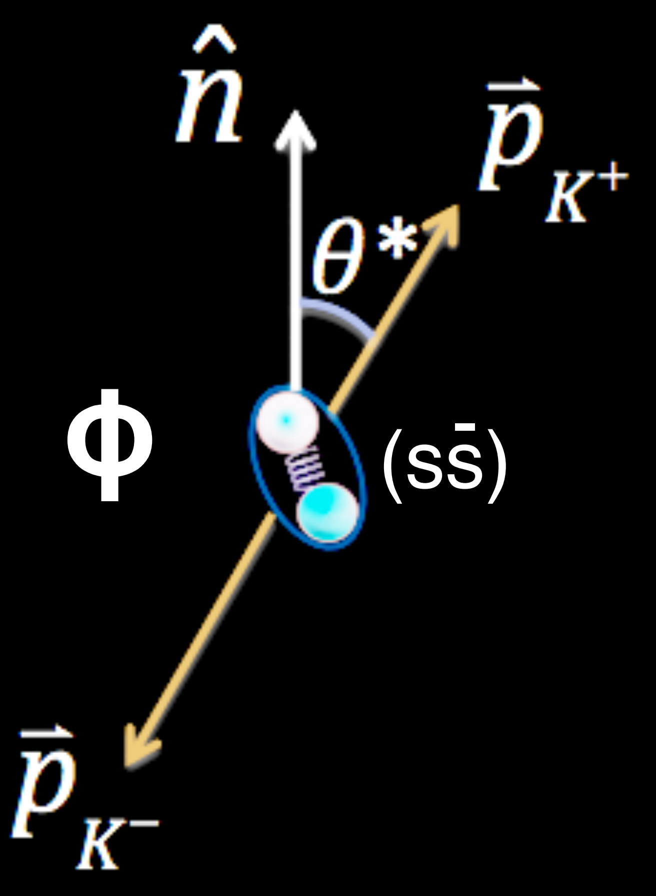

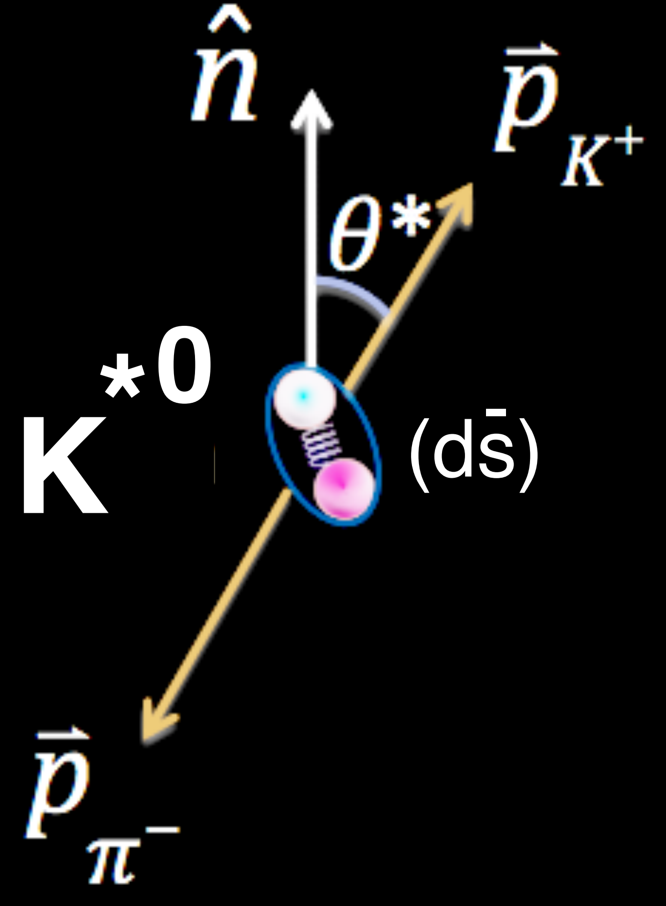

K^{*0} meson consistent with 1/3

8.4σ positive deviation from 1/3 for φ meson

M. Abdallah et al (STAR Collaboration), arXiv: 2204:XXYY

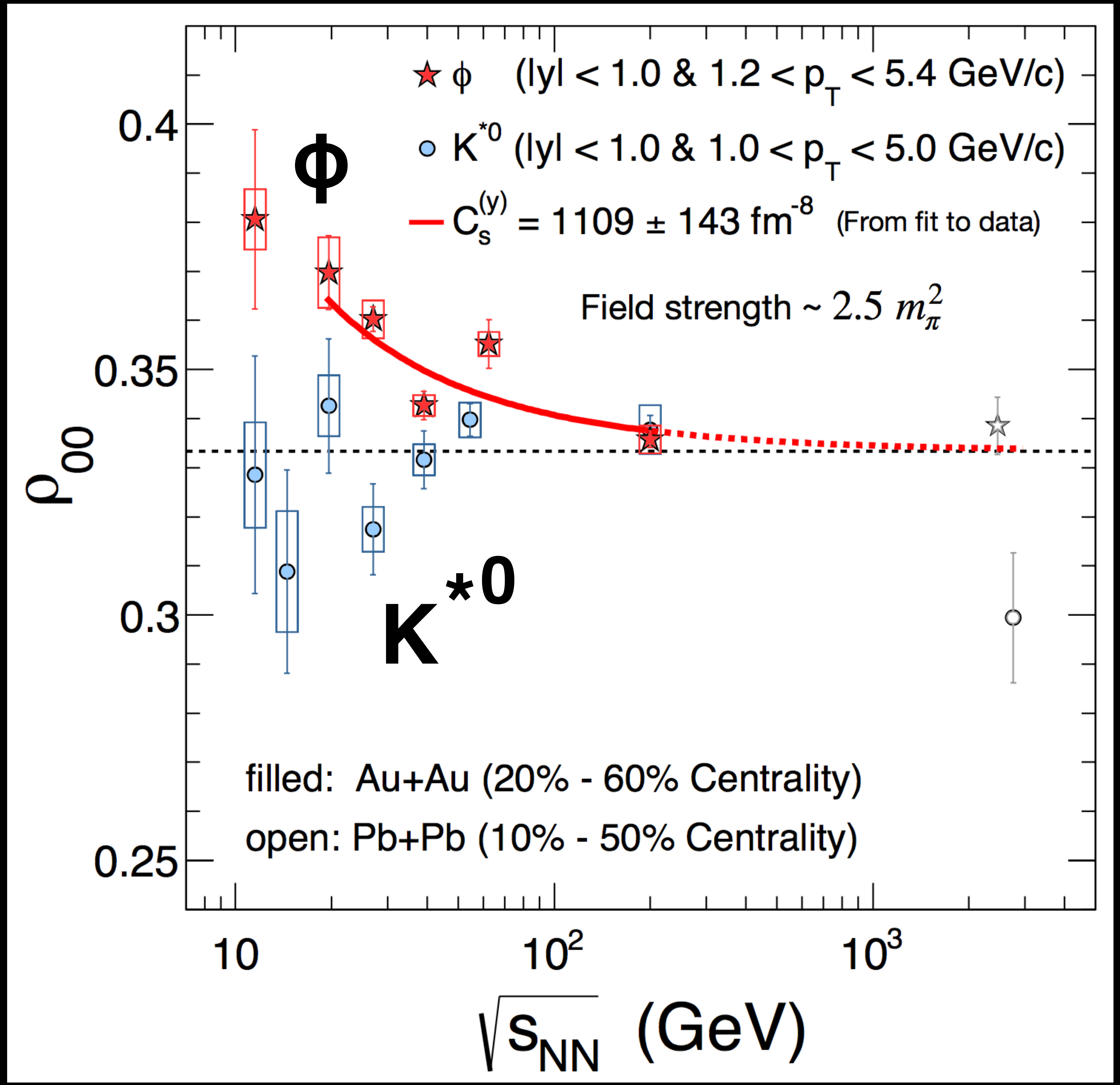

What causes vector meson spin alignment? Strong force field?

Like Λ polarization (-10^{-5}) Electric field (-10^{-4})

$$\rho_{00}^{\phi} \approx \frac{1}{3} + c_\Lambda + c_\varepsilon + c_E + c_\phi$$

Vorticity tensor (-10^{-4}) Vector meson field

Sheng et al, Phys. Rev. D 101 096005 (2020), Phys. Rev. D 102, 056013 (2020)

Charged $K^{*\pm}$ measurements in will provide more insights

Model with strong vector meson force field (~2.5 m_π^2) provides a possible explanation